



Analytical solutions for functionally graded incompressible eccentric and non-axisymmetrically loaded circular cylinders

R.C. Batra^{a,*}, G.J. Nie^{b,a}

^a Department of Engineering Science and Mechanics, M/C 0219, Virginia Polytechnic Institute and State University, Blacksburg, VA 24061, United States

^b School of Aerospace Engineering and Applied Mechanics, Tongji University, Shanghai 200092, China

ARTICLE INFO

Article history:

Available online 14 November 2009

Keywords:

Eccentric cylinders
Non-axisymmetric loads
Functionally graded rubberlike materials

ABSTRACT

We study analytically plane strain static deformations of functionally graded eccentric and non-axisymmetrically loaded circular cylinders comprised of isotropic and incompressible linear elastic materials. Normal and tangential surface tractions on the inner and the outer surfaces of a cylinder may vary in the circumferential direction. The shear modulus is taken to vary either as an exponential function or as a power law function of the radius only. The radial and the circumferential displacements, and the hydrostatic pressure are expanded in Fourier series in the angular coordinate, and expressions for their coefficients are derived from equations expressing the balance of mass (or the continuity equation) and the balance of linear momentum. Boundary conditions are satisfied in the sense of Fourier series. For the exponential variation of the shear modulus, the method of Frobenius series is used to solve 4th-order ordinary differential equations for coefficients of the Fourier series. It is shown that the series solutions for displacements and the hydrostatic pressure converge rapidly. Results for eccentric cylinders and non-axisymmetrically loaded circular cylinders are computed and exhibited graphically. Effects on stress distributions of the eccentricity in the cylinders and of the gradation in the shear modulus are illuminated. It is found that in a thin cylinder subjected to sinusoidally varying pressure on the inner surface, segments of the cylinder between two adjacent cusps in the pressure deform due to bending rather than stretching.

© 2009 Elsevier Ltd. All rights reserved.

1. Introduction

One way to optimally design hollow cylindrical structures is to suitably vary material properties in them so as to optimize a design variable such as the maximum principal stress, the maximum shear stress, the cylinder thickness, and the eccentricity between the inner and the outer circular surfaces of the cylinder. The tailored material properties can be obtained either by fabricating the structure from more than one material and varying their volume fractions or by changing the molecular and the chemical structure by exposing the material to either ultraviolet light or appropriate heat and chemical treatments. Materials with continuously varying elastic moduli are usually called functionally graded (FG), and structures comprised of such materials are termed FG structures (FGSs). Advantages of FGSs over laminated composites include the elimination of interfaces between different constituents/layers thereby avoiding points of high stress concentration. However, FGSs fabricated by continuously varying volume fractions of reinforcing particulates in a matrix may have too many surfaces where debonding between particulates and the matrix

can occur. For mathematical considerations FGSs are comprised of inhomogeneous materials.

Rubberlike and polymeric materials are extensively used in every day life, e.g., tires, hoses, seals in automotive and aerospace applications, reinforcements for soft biological tissues, etc. Rubberlike materials are usually regarded as incompressible. An incompressible material can undergo only isochoric or volume preserving deformations and accordingly its constitutive relation has a hydrostatic pressure that cannot be determined from the deformation field but is to be found as a part of the solution of the boundary-value problem.

Solutions to linear elastic problems for inhomogeneous materials are given in Lekhnitskii's book [1]. A general theory of nonlinear elastic problems can be found in Truesdell and Noll's book [2]. Linear elastic axisymmetric problems for FG cylinders comprised of compressible materials have been studied in [3–13], and for incompressible materials in [14]. Finite deformations of axisymmetrically loaded FG cylinders comprised of Mooney–Rivlin and 2nd-order elastic incompressible materials have been analyzed in [15–18]. However, non-axisymmetric problems for circular cylinders, and boundary-value problems for eccentric cylinders have received very little attention. During the Couette flow of a viscous fluid between two cylinders, the fluid exerts both tangential and

* Corresponding author. Tel.: +1 5402316051; fax: +1 5402314574.
E-mail address: rbatra@vt.edu (R.C. Batra).

normal surface tractions on the cylinders surfaces, and eccentricities between the inner and the outer surfaces during the fabrication of a hollow cylinder are generally unavoidable. A partially filled pressure vessel has tractions acting only on a part of the inner surface. The literature search on scholar.google.com revealed numerous works related to the flow of fluids between eccentric cylinders. The analysis of these problems is more challenging than that of axisymmetric problems because the radial and the circumferential components of displacements and the hydrostatic pressure need to be found as a function of r and θ where (r, θ) denotes cylindrical coordinates of a point with the origin of the axes at the center of the inner circular surface. Here we study analytically static deformations of a FG hollow circular cylinder with non-axisymmetric tractions applied to its inner and outer surfaces, and of an eccentric cylinder under similar loads. In each case, the cylinder material is linear elastic and incompressible. We note that a linear thermoelastic problem for a thick FG circular cylinder with constant Poisson's ratio, and Young's modulus and the coefficient of thermal expansion given by power law functions of the radial coordinate and non-axisymmetric loads prescribed on the inner surface has been analyzed in [19]. The current work differs from that reported in [19] in several respects. For example, the hydrostatic pressure is found by satisfying the continuity condition, exponential variation of the shear modulus in the radial direction is considered, problems for circular cylinders with tangential tractions applied to its bounding surfaces are studied, and deformations of a thin cylinder with the pressure applied on the inner surface varying sinusoidally, stress concentration in a thick cylinder loaded by a periodic pressure on the outer surface, and problems for eccentric cylinders have been scrutinized. The analysis of a problem for a cylinder with the exponential variation of the shear modulus is more involved than that of the same problem when the shear modulus varies according to a power law relation.

2. Problem formulation

Consider an infinitely long hollow cylinder of uniform cross-section of inner radius r_{in} , outer radius r_{ou} and the inner and the outer circular surfaces having an eccentricity e as shown in Fig. 1. We take the origin of the cylindrical coordinate axes at the center of the inner circular surface, and denote coordinates of a point by (r, θ, z) . The cylinder is made of an incompressible and isotropic linear elastic material with the shear modulus assumed to vary in the radial direction either by a power-law or an exponential function. The cylinder is loaded by pressures $p_{in}(\theta)$, $p_{ou}(\theta)$ and tangential tractions $q_{in}(\theta)$ and $q_{ou}(\theta)$, respectively, on its inner and outer surfaces (cf. Fig. 1). Alternatively, the radial and the circumferential displacements could be prescribed at one or both of these bounding surfaces as for the rectilinear shear deformations studied in [18]. Because the shear modulus, the cylinder geometry, and the applied loads are independent of the axial coordinate z of a point, the state of deformation in the cylinder is that of plane

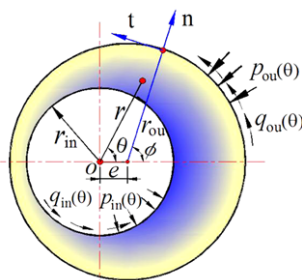


Fig. 1. Schematic sketch of the problem studied.

strain, and stresses and strains are independent of the z -coordinate.

Equations of equilibrium in polar coordinates (r, θ) , in the absence of body forces, are

$$\begin{aligned} \frac{\partial \sigma_{rr}}{\partial r} + \frac{1}{r} \frac{\partial \sigma_{r\theta}}{\partial \theta} + \frac{\sigma_{rr} - \sigma_{\theta\theta}}{r} &= 0, \\ \frac{\partial \sigma_{\theta r}}{\partial r} + \frac{1}{r} \frac{\partial \sigma_{\theta\theta}}{\partial \theta} + \frac{2}{r} \sigma_{\theta r} &= 0, \end{aligned} \quad r_{in} < r < \tilde{r}(\theta), \tag{1}$$

where σ_{rr} , $\sigma_{r\theta} = \sigma_{\theta r}$ and $\sigma_{\theta\theta}$ are components of the stress tensor, $r = r_{in}$ on the inner surface, and $r = \tilde{r}(\theta)$ describes the outer bounding surface of the cylinder. The function $\tilde{r}(\theta)$ is given by

$$\tilde{r}(\theta) = e \cos \theta + \sqrt{-e^2 \sin^2 \theta + r_{ou}^2},$$

where e is the eccentricity between the inner and the outer circular surfaces of the cylinder and r_{ou} the radius of the outer circular surface; cf. Fig. 1.

The non-zero components of the infinitesimal strain tensor are given by

$$\begin{aligned} e_{rr} &= u_{r,r}, \quad e_{\theta\theta} = \frac{1}{r} u_r + \frac{1}{r} u_{\theta,\theta}, \\ 2e_{r\theta} &= 2e_{\theta r} = \frac{1}{r} u_{r,\theta} + u_{\theta,r} - \frac{1}{r} u_{\theta}, \quad u_{r,r} = \frac{\partial u_r}{\partial r}, \quad u_{\theta,\theta} = \frac{\partial u_\theta}{\partial \theta}, \end{aligned} \tag{2}$$

where u_r and u_θ are physical components of the displacement \mathbf{u} in the radial and the circumferential directions, respectively.

Since only isochoric (volume preserving) deformations are admissible in an incompressible material, therefore, displacements must satisfy

$$e_{rr} + e_{\theta\theta} = 0, \quad r_{in} < r < \tilde{r}(\theta). \tag{3}$$

The constitutive equation for an incompressible and isotropic linear elastic material is

$$\boldsymbol{\sigma} = -p\mathbf{1} + 2\mu(r)\mathbf{e}, \tag{4}$$

where p is the hydrostatic pressure not determined from the deformation field, $\mathbf{1}$ is the identity tensor, and $\mu(r)$ is the shear modulus. The pertinent boundary conditions are

$$\begin{aligned} \sigma_{rr}(r_{in}, \theta) &= -p_{in}(\theta) \quad \text{or} \quad u_r(r_{in}, \theta) = \bar{u}_r^{in}(\theta), \\ \sigma_{r\theta}(r_{in}, \theta) &= -q_{in}(\theta) \quad \text{or} \quad u_\theta(r_{in}, \theta) = \bar{u}_\theta^{in}(\theta), \quad \text{(a-d)} \\ \sigma_{rr}(\tilde{r}(\theta), \theta) \cos(\phi - \theta) &+ \sigma_{r\theta}(\tilde{r}(\theta), \theta) \sin(\phi - \theta) \\ &= -p_{ou}(\theta) \cos(\phi - \theta) + q_{ou}(\theta) \sin(\phi - \theta), \quad \text{or} \\ u_r(\tilde{r}(\theta), \theta) &= \bar{u}_r^{ou}(\theta) \quad \text{(e, f)} \\ \sigma_{r\theta}(\tilde{r}(\theta), \theta) \cos(\phi - \theta) &+ \sigma_{\theta\theta}(\tilde{r}(\theta), \theta) \sin(\phi - \theta) \\ &= -p_{ou}(\theta) \sin(\phi - \theta) + q_{ou}(\theta) \cos(\phi - \theta), \quad \text{or} \\ u_\theta(\tilde{r}(\theta), \theta) &= \bar{u}_\theta^{ou}(\theta), \quad \text{(g, h)} \end{aligned} \tag{5}$$

where

$$r_{ou} \sin \phi = \tilde{r}(\theta) \sin \theta. \tag{6}$$

In Eqs. (5b,d,f,h) a superposed bar on \mathbf{u} indicates that the value of the function is specified, superscripts and subscripts 'in' and 'ou' affixed to a quantity indicate, respectively, the value of the quantity at the inner and the outer surfaces of the cylinder, and subscripts 'r' and ' θ ' on a quantity indicate its value in the radial and the circumferential directions, respectively. When only surface tractions are prescribed on the bounding surfaces, then values of $q_{in}(\theta)$, $p_{ou}(\theta)$ and $q_{ou}(\theta)$ must be such that the cylinder is in equilibrium under the application of external loads. That is,

$$\int_0^{2\pi} q_{in}(\theta) r_{in}^2 d\theta + \int_0^{2\pi} \tilde{r}^2(\theta) [-p_{ou}(\theta) \sin(\phi - \theta) + q_{ou}(\theta) \cos(\phi - \theta)] d\theta = 0. \tag{7}$$

3. Analytical solution

We assume that the displacement and the hydrostatic pressure fields can be expressed as

$$u_r(r, \theta) = \sum_{m=0}^{\infty} [u_{rm}^c(r)\varphi_m^c + u_{rm}^s(r)\varphi_m^s], \tag{8a}$$

$$u_{\theta}(r, \theta) = \sum_{m=0}^{\infty} [u_{\theta m}^c(r)\varphi_m^c + u_{\theta m}^s(r)\varphi_m^s], \tag{8b}$$

$$p(r, \theta) = \sum_{m=0}^{\infty} [p_m^c(r)\varphi_m^c + p_m^s(r)\varphi_m^s], \tag{8c}$$

where the integer m equals the circumferential wave number, $\varphi_m^c = \cos(m\theta)$, $\varphi_m^s = \sin(m\theta)$, and superscripts c and s signify, respectively, quantities associated with the cosine and the sine terms. For radial expansion/contraction of a circular cylinder due to pressures applied to its inner and outer surfaces, $u_{r0}^c \neq 0$, $p_0^c \neq 0$, and coefficients of the remaining cosine and the sine terms in Eq. (8) can be taken as zeros; e.g. see the analysis presented in [14]. For non-axisymmetric problems, we take $u_{r0}^s = u_{\theta 0}^s = p_0^s = 0$ since they do not contribute to u_r , u_{θ} and p respectively.

Substitution for displacements u_r and u_{θ} from Eq. (8) into Eqs. (2) and (3), and equating to zero coefficients of $\cos(m\theta)$ and $\sin(m\theta)$ we obtain

$$\begin{aligned} (u_{rm,r}^c + \frac{1}{r}u_{rm}^c - \frac{m}{r}u_{\theta m}^s) &= 0, \quad m = 0, 1, 2, \dots, \\ (u_{rm,r}^s + \frac{1}{r}u_{rm}^s - \frac{m}{r}u_{\theta m}^c) &= 0, \quad m = 1, 2, \dots \end{aligned} \tag{9a, b}$$

Thus for $m \neq 0$,

$$u_{\theta m}^s = -\frac{1}{m}(ru_{rm,r}^c), \quad u_{\theta m}^c = \frac{1}{m}(ru_{rm,r}^s), \tag{10a, b}$$

and for $m = 0$, we get from Eq. (9a)

$$u_{r0}^c = \frac{a_{r0}^c}{r}, \tag{10c}$$

where a_{r0}^c is a constant.

Substituting for u_r , u_{θ} and p from Eq. (8) into Eqs. (2), (4), and (1) we get

$$\begin{aligned} \sum_{m=0}^{\infty} [g_{1m}(r)\varphi_m^c + g_{2m}(r)\varphi_m^s] &= \sum_{m=0}^{\infty} [p_{m,r}^c(r)\varphi_m^c + p_{m,r}^s(r)\varphi_m^s], \\ \sum_{m=0}^{\infty} [g_{3m}(r)\varphi_m^c + g_{4m}(r)\varphi_m^s] &= \sum_{m=0}^{\infty} \frac{m}{r} [-p_m^c(r)\varphi_m^s + p_m^s(r)\varphi_m^c], \end{aligned} \tag{11}$$

where

$$\begin{aligned} g_{1m}(r) &= \mu(r) \left(2u_{rm,rr}^c + \frac{2}{r}u_{rm,r}^c - \frac{2+m^2}{r^2}u_{rm}^c + \frac{m}{r}u_{\theta m,r}^s - \frac{3m}{r^2}u_{\theta m}^s \right) \\ &\quad + 2\mu_{,r}(r)u_{rm,r}^c, \\ g_{2m}(r) &= \mu(r) \left(2u_{rm,rr}^s + \frac{2}{r}u_{rm,r}^s - \frac{2+m^2}{r^2}u_{rm}^s - \frac{m}{r}u_{\theta m,r}^c + \frac{3m}{r^2}u_{\theta m}^c \right) \\ &\quad + 2\mu_{,r}(r)u_{rm,r}^s, \\ g_{3m}(r) &= \frac{\mu(r)}{r^2} (r^2u_{\theta m,rr}^c + r(u_{\theta m,r}^c + mu_{rm,r}^s) - (2m^2 + 1)u_{\theta m}^c + 3mu_{rm}^s) \\ &\quad + \frac{\mu_{,r}(r)}{r} (mu_{rm}^s - u_{\theta m}^c + ru_{\theta m,r}^c), \\ g_{4m}(r) &= \frac{\mu(r)}{r^2} (r^2u_{\theta m,rr}^s + r(u_{\theta m,r}^s - mu_{rm,r}^c) - (2m^2 + 1)u_{\theta m}^s - 3mu_{rm}^c) \\ &\quad - \frac{\mu_{,r}(r)}{r} (mu_{rm}^c + u_{\theta m}^s - ru_{\theta m,r}^s). \end{aligned} \tag{12}$$

Equating coefficients of $\cos(m\theta)$ and $\sin(m\theta)$ on both sides of Eq. (11) gives

$$g_{1m}(r) = p_{m,r}^c, \quad g_{2m}(r) = p_{m,r}^s, \quad rg_{4m}(r) = -mp_m^c, \quad rg_{3m}(r) = mp_m^s. \tag{13a-d}$$

Thus for $m \neq 0$, we get the following compatibility conditions for the pressure field, p , to exist:

$$mg_{1m} = -(rg_{4m})_{,r}, \quad mg_{2m} = (rg_{3m})_{,r}. \tag{14a, b}$$

For $m = 0$, it follows from Eqs. (13c) and (13d) that $g_{30}(r) = 0$, $g_{40}(r) = 0$. Recalling that $u_{\theta 0}^s = 0$, thus u_{r0}^c is the solution of the following ordinary differential equation:

$$\mu(r) \left(u_{r0,rr}^c + \frac{1}{r}u_{r0,r}^c - \frac{1}{r^2}u_{r0}^c \right) + \mu_{,r}(r) \left(u_{\theta 0,r}^c - \frac{1}{r}u_{\theta 0}^c \right) = 0. \tag{15}$$

For an inhomogeneous cylinder, as should be clear from Eq. (10c), u_{r0}^c is independent of the variation of the shear modulus; however, $u_{\theta 0}^c$ may depend upon the variation with the radius r of the shear modulus. Because the component p_0^s of the hydrostatic pressure is taken to be zero, the component p_0^c is the solution of Eq. (13a), viz.,

$$p_{0,r}^c = 2\mu(r) \left(u_{r0,rr}^c + \frac{1}{r}u_{r0,r}^c - \frac{1}{r^2}u_{r0}^c \right) + 2\mu_{,r}(r)u_{r0,r}^c. \tag{16}$$

Substitution for u_{r0}^c from Eq. (10c) into Eq. (16), and integration of the resulting equation give

$$p_0^c = b_0^c - 2a_{r0}^c \int_{r_{in}}^r \frac{\mu_{,y}(y)}{y^2} dy, \tag{17}$$

where b_0^c is a constant.

For $m = 0$, u_{r0}^c is given by Eq. (10c), p_0^c is computed from Eq. (17), and $u_{\theta 0}^c$ is found by solving Eq. (15). Thus there are four constants of integration to be determined from the boundary conditions.

For $m \neq 0$, u_{rm}^c and u_{rm}^s are solutions of ordinary differential Eqs. (14a) and (14b), $u_{\theta m}^c$ and $u_{\theta m}^s$ are determined, respectively, from Eqs. (10a) and (10b), and p_m^c and p_m^s are given by Eqs. (13c) and (13d), respectively. Thus constants appearing in expressions for p_m^c , p_m^s , $u_{\theta m}^c$ and $u_{\theta m}^s$ are the same as those in the expressions for u_{rm}^c and u_{rm}^s . Substitution for $u_{\theta m}^c$ and $u_{\theta m}^s$ from Eqs. (10a) and (10b) into Eqs. (14a) and (14b) gives 4th-order ordinary differential equations for u_{rm}^c and u_{rm}^s ; e.g. see Eq. (21) below. Hence expressions for u_{rm}^c and u_{rm}^s will each have four constants of integration. For M terms retained in series solution (8), there are $(8M - 4)$ unknowns to be determined since there are only four constants of integration for $m = 0$. These are found by satisfying boundary conditions (5) in the sense of Fourier series. For example, both sides of Eq. (5a) are multiplied with $\varphi_l^c = \cos(l\theta)$ and $\varphi_l^s = \sin(l\theta)$, and the resulting equations integrated over $(0, 2\pi)$ with the following result:

$$\int_0^{2\pi} \sigma_{rr}(r_{in}, \theta)\varphi_l^c d\theta = - \int_0^{2\pi} p_{in}(\theta)\varphi_l^c d\theta, \quad l = 0, 1, 2, \dots \tag{18a, b}$$

For each non-zero value of l , boundary conditions on the inner surface give four algebraic equations, and those on the outer surface also give four algebraic equations. For M terms in the series solution (8), we use M sequential integer values of l in Eq. (18) resulting in the number of algebraic equations equal to the number of unknowns in expression (8a) for u_r .

Having found the displacement and the pressure fields, strains are computed from Eq. (2) and then stresses from Eq. (4). We note that for the shear modulus $\mu > 0$, the solution of the boundary-value problem in linear elasticity is unique within a rigid body motion.

3.1. Cylinder made of a homogeneous material

For a cylinder comprised of a homogeneous material, $\mu_{,r} = 0$, and Eqs. (15) and (17) give

$$u_{\theta 0}^c = \frac{a_{\theta 0}^c}{r} + b_{\theta 0}^c r, \quad p_0^c = b_0^c, \tag{19}$$

where $a_{\theta 0}^c$ and $b_{\theta 0}^c$ are constants. Thus Eq. (8) can be written as

$$\begin{aligned} u_r(r, \theta) &= \frac{a_{r0}^c}{r} + \sum_{m=1}^{\infty} [u_{rm}^c(r)\varphi_m^c + u_{rm}^s(r)\varphi_m^s], \\ u_{\theta}(r, \theta) &= \frac{a_{\theta 0}^c}{r} + b_{\theta 0}^c r + \sum_{m=1}^{\infty} [u_{\theta m}^c(r)\varphi_m^c + u_{\theta m}^s(r)\varphi_m^s], \\ p(r, \theta) &= b_0^c + \sum_{m=1}^{\infty} [p_m^c(r)\varphi_m^c + p_m^s(r)\varphi_m^s]. \end{aligned} \tag{20}$$

For $m \geq 1$, Eqs. (14a) and (14b) after substitutions for $u_{\theta m}^c$ and $u_{\theta m}^s$ from Eqs. (10a) and (10b) give identical 4th-order ordinary differential equations for u_{rm}^c and u_{rm}^s ; that for u_{rm}^c is given below:

$$r^4 u_{rm,rrrr}^c + 6r^3 u_{rm,rrr}^c - (2m^2 - 5)r^2 u_{rm,rr}^c - (2m^2 + 1)r u_{rm,r}^c + (m^2 - 1)^2 u_{rm}^c = 0. \tag{21}$$

Since the coefficient of u_{rm}^c vanishes for $m = 1$, we give below solutions of Eq. (21) for $m = 1$, and $m > 1$. For $m = 1$, the solution of Eq. (21) is

$$\begin{aligned} u_{r1}^{\alpha} &= -\frac{c_{11}^{\alpha}}{r^2} + c_{21}^{\alpha} \ln r + c_{31}^{\alpha} r^2 + c_{41}^{\alpha}, \quad \alpha = c, s, \\ u_{\theta 1}^c &= \frac{c_{11}^c}{r^2} + c_{21}^c (1 + \ln r) + 3c_{31}^c r^2 + c_{41}^c, \\ u_{\theta 1}^s &= -\frac{c_{11}^s}{r^2} - c_{21}^s (1 + \ln r) - 3c_{31}^s r^2 - c_{41}^s, \\ p_1^{\alpha} &= \mu_0 \left(-\frac{2c_{21}^{\alpha}}{r} + 8rc_{31}^{\alpha} \right), \quad \alpha = c, s. \end{aligned} \tag{22}$$

For $m > 1$, we get the following for the solution of Eq. (21):

$$\begin{aligned} u_{rm}^{\alpha} &= c_{1m}^{\alpha} r^{-1-m} + c_{2m}^{\alpha} r^{1-m} + c_{3m}^{\alpha} r^{1+m} + c_{4m}^{\alpha} r^{-1+m}, \quad \alpha = c, s, \\ u_{\theta m}^c &= -c_{1m}^c r^{-1-m} + \left(\frac{2}{m} - 1 \right) c_{2m}^c r^{1-m} \\ &\quad + \left(\frac{2}{m} + 1 \right) c_{3m}^c r^{1+m} + c_{4m}^c r^{-1+m}, \\ u_{\theta m}^s &= c_{1m}^s r^{-1-m} + \left(1 - \frac{2}{m} \right) c_{2m}^s r^{1-m} \\ &\quad - \left(\frac{2}{m} + 1 \right) c_{3m}^s r^{1+m} - c_{4m}^s r^{-1+m}, \\ p_m^{\alpha} &= \frac{4\mu_0 r^{-m}}{m} [(m-1)c_{2m}^{\alpha} + (m+1)r^2 c_{3m}^{\alpha}], \quad \alpha = c, s, \end{aligned} \tag{23}$$

where $c_{1m}^{\alpha}, c_{2m}^{\alpha}, c_{3m}^{\alpha}$ and c_{4m}^{α} ($\alpha = c, s$) are constants of integration to be determined from the boundary conditions.

3.2. Cylinder composed of a FGM

3.2.1. Power-law variation of the shear modulus

We assume that the shear modulus, $\mu(r)$, is given by

$$\mu(r) = \mu_0 \left(\frac{r}{r_{ou}} \right)^n, \tag{24}$$

where μ_0 is the reference value of the shear modulus, and the exponent n describes the variation in the radial direction of the shear modulus. For a cylinder made of a homogeneous material $n = 0$. For $n > 0$, the shear modulus increases monotonically from its value $\mu_0(r_{in}/r_{ou})^n$ at points on the inner surface to $\mu_0(\bar{r}(\theta)/r_{ou})^n$ at points on the outer periphery of the cylinder. For $n < 0$, the shear modulus has the largest value at points on the inner surface of the cylinder. Since the radial coordinate of a point on the exterior boundary is a function of r_{ou} and θ , therefore, the shear modulus appears to depend upon r and θ even though there is no explicit dependence of μ upon θ in Eq. (24). As for a cylinder made of a homogeneous mate-

rial, ordinary differential equations for finding u_{rm} when $m = 0, m = 1$ and $m > 1$ are different. Accordingly, we list below solutions for these three cases. In the remainder of this sub-section we have assumed that $n \neq 0$.

For $m = 0$, substitution for $\mu(r)$ from Eq. (24) into Eq. (15) gives a 2nd-order ordinary differential equation for $u_{\theta 0}$. For $n \neq -1$, the solution is

$$u_{\theta 0}^c = a_{\theta 0}^c r + b_{\theta 0}^c r^{-(n+1)} \tag{25}$$

and for $n = -1$, we have

$$u_{\theta 0}^c = a_{\theta 0}^c + b_{\theta 0}^c r, \tag{26}$$

where $a_{\theta 0}^c$ and $b_{\theta 0}^c$ are constants of integration. Similarly, substituting for $\mu(r)$ from Eq. (24) into Eq. (17) and simplification of the resulting equation gives the following expression for the hydrostatic pressure.

For $n \neq 2$,

$$p_0^c = b_0^c - 2a_{r0}^c \frac{\mu_0}{r^2} \frac{n}{n-2} \left(\frac{r}{r_{ou}} \right)^n. \tag{27}$$

For $n = 2$,

$$p_0^c = b_0^c - 4a_{r0}^c \frac{\mu_0}{r_{ou}^2} \ln r. \tag{28}$$

For $m = 1$, expressions for displacements and the hydrostatic pressure are

$$\begin{aligned} u_{r1}^{\alpha} &= \frac{c_{11}^{\alpha}}{8} n_{t1} r^{-\frac{1}{2}n_{t2}} + \frac{c_{21}^{\alpha}}{8} n_{t2} r^{-\frac{1}{2}n_{t1}} - \frac{c_{31}^{\alpha}}{n} r^{-n} + c_{41}^{\alpha}, \quad \alpha = c, s, \\ u_{\theta 1}^c &= \frac{c_{11}^c}{8} (n_{t1} + 8) r^{-\frac{1}{2}n_{t2}} + \frac{c_{21}^c}{8} (n_{t2} + 8) r^{-\frac{1}{2}n_{t1}} + \frac{c_{31}^c (n-1)}{n} r^{-n} + c_{41}^c, \\ u_{\theta 1}^s &= -\frac{c_{11}^s}{8} (n_{t1} + 8) r^{-\frac{1}{2}n_{t2}} - \frac{c_{21}^s}{8} (n_{t2} + 8) r^{-\frac{1}{2}n_{t1}} - \frac{c_{31}^s (n-1)}{n} r^{-n} - c_{41}^s, \\ p_1^{\alpha} &= \mu_0 \left(\frac{r}{r_{ou}} \right)^n \left(\frac{c_{11}^{\alpha}}{2} (4 - n_{t2}) r^{(-1-\frac{1}{2}n_{t2})} + \frac{c_{21}^{\alpha}}{2} (4 - n_{t1}) r^{(-1-\frac{1}{2}n_{t1})} \right. \\ &\quad \left. - c_{31}^{\alpha} (n+2) r^{-1-n} \right), \alpha = c, s, \end{aligned} \tag{29a - d}$$

where $n_{t1} = n - \sqrt{16 + n^2}$, and $n_{t2} = n + \sqrt{16 + n^2}$.

For $m \geq 2$, displacements and the hydrostatic pressure are given by

$$\begin{aligned} u_{rm}^{\alpha} &= \sum_{i=1}^4 c_{im}^{\alpha} r^{n_i}, \quad \alpha = c, s, \\ u_{\theta m}^c &= \sum_{i=1}^4 \frac{c_{im}^c (1 + n_i) r^{n_i}}{m}, \quad u_{\theta m}^s = -\sum_{i=1}^4 \frac{c_{im}^s (1 + n_i) r^{n_i}}{m}, \\ p_m^{\alpha} &= \mu_0 \left(\frac{r}{r_{ou}} \right)^n \sum_{i=1}^4 \tilde{C}_{im}^{\alpha} r^{n_i-1}, \quad \alpha = c, s, \end{aligned} \tag{30a - d}$$

where $\tilde{C}_{im}^{\alpha} = c_{im}^{\alpha} (1 + n - n_i) + c_{im}^{\alpha} (1 + n + n_i) (n_i^2 - 1) / m^2$, c_{im}^{α} ($\alpha = c, s, i = 1, 2, 3, 4$) are constants of integration to be determined from the boundary conditions, and

$$\begin{aligned} n_1 &= \frac{1}{2} \left(-n - \sqrt{n_{m1} - 4\sqrt{n_{m2}}} \right), \quad n_2 = \frac{1}{2} \left(-n + \sqrt{n_{m1} - 4\sqrt{n_{m2}}} \right), \\ n_{m1} &= 4 + 4m^2 + n^2, \\ n_3 &= \frac{1}{2} \left(-n - \sqrt{n_{m1} + 4\sqrt{n_{m2}}} \right), \quad n_4 = \frac{1}{2} \left(-n + \sqrt{n_{m1} + 4\sqrt{n_{m2}}} \right), \\ n_{m2} &= 4m^2 + n^2 - m^2 n^2. \end{aligned} \tag{31}$$

3.2.2. Exponential variation of the shear modulus

The exponential variation of the shear modulus is assumed to be given by the following equation:

$$\mu(r) = \mu_0 \exp(\beta r), \tag{32}$$

where $\mu_0 = \tilde{\mu}_0 \exp(-\tilde{\beta})$ and $\beta = \tilde{\beta}/r_{ou}$ control the variation of the shear modulus in the radial direction and $\tilde{\mu}_0$ equals the shear modulus at a point on the outer surface of the cylinder. For a cylinder made of a homogeneous material $\beta = 0$.

As for the power-law variation of the shear modulus, we consider separately cases when $m = 0$, $m = 1$ and $m > 1$.

For $m = 0$, substitution for $\mu(r)$ from Eq. (32) into Eq. (15) gives the following 2nd-order differential equation for $u_{\theta 0}^c$:

$$r^2 u_{\theta 0,rr}^c + r u_{\theta 0,r}^c - u_{\theta 0}^c + \beta r (r u_{\theta 0,r}^c - u_{\theta 0}^c) = 0. \tag{33}$$

Thus

$$u_{\theta 0}^c = a_{\theta 0}^c r + \frac{b_{\theta 0}^c e^{-\beta r}}{4r} (\beta^2 e^{\beta r} r^2 \text{Ei}(-\beta r) + \beta r - 1), \tag{34}$$

where $\text{Ei}(-\beta r)$ is the exponential integral function.

Substitution for $\mu(r)$ from Eq. (32) into Eq. (17) yields

$$p_0^c = b_0^c - 2\beta a_{r0}^c f(r), f(r) = \int_{r_{in}}^r \frac{\mu_0 e^{\beta y}}{y^2} dy. \tag{35}$$

For $m = 1$, the differential equation for the radial displacement is

$$u_{r1,rrr}^{\alpha} + \left(2\beta + \frac{6}{r}\right) u_{r1,rr}^{\alpha} + \left(\beta^2 + \frac{7\beta}{r} + \frac{3}{r^2}\right) u_{r1,r}^{\alpha} + \left(\frac{\beta^2}{r} - \frac{\beta}{r^2} - \frac{3}{r^3}\right) u_{r1}^{\alpha} = 0, \quad \alpha = c, s. \tag{36}$$

The analytical solution of Eq. (36) is

$$u_{r1}^{\alpha} = C_{11}^{\alpha} f_{r1} + C_{21}^{\alpha} f_{r2} + C_{31}^{\alpha} f_{r3} + C_{41}^{\alpha}, \quad \alpha = c, s. \tag{37}$$

Expressions for f_{ri} ($i = 1, 2, 3$) are given in Appendix A.

Substitution from Eq. (37) into Eqs. (10), (13c) and (13d) gives

$$\begin{aligned} u_{\theta 1}^{\alpha} &= C_{11}^{\alpha} f_{\theta 1} + C_{21}^{\alpha} f_{\theta 2} + C_{31}^{\alpha} f_{\theta 3} - C_{41}^{\alpha}, \\ u_{\theta 1}^c &= -C_{11}^c f_{\theta 1} - C_{21}^c f_{\theta 2} - C_{31}^c f_{\theta 3} + C_{41}^c, \\ p_1^{\alpha} &= \mu_0 \exp(\beta r) (C_{11}^{\alpha} f_{p1} + C_{21}^{\alpha} f_{p2} + C_{31}^{\alpha} f_{p3}), \quad \alpha = c, s. \end{aligned} \tag{38}$$

Expressions for $f_{\theta i}$ and $f_{p i}$ ($i = 1, 2, 3$) are given in Appendix A.

For $m \geq 2$, the 4th-order differential equation for the radial displacement is

$$\begin{aligned} u_{rm,rrrr}^{\alpha} + \left(2\beta + \frac{6}{r}\right) u_{rm,rrr}^{\alpha} + \left(\beta^2 + \frac{7\beta}{r} + \frac{5-2m^2}{r^2}\right) u_{rm,rr}^{\alpha} \\ + \left(\frac{\beta^2}{r} + \frac{\beta(1-2m^2)}{r^2} - \frac{1+2m^2}{r^3}\right) u_{rm,r}^{\alpha} \\ + \left(\frac{\beta^2}{r^2} + \frac{\beta}{r^3} + \frac{m^2-1}{r^4}\right) (m+1)(m-1) u_{rm}^{\alpha} = 0, \quad \alpha = c, s. \end{aligned} \tag{39}$$

Eq. (39) is solved using the Frobenius series method. The series solution of Eq. (39) is taken to be

$$u_{rm}^{\alpha}(r) = \sum_{k=0}^{\infty} a_k^{\alpha} r^{k+t}, \quad a_0^{\alpha} \neq 0 \quad \text{and} \quad \alpha = c, s, \tag{40}$$

where the exponent t is to be determined, and a_k^{α} is a constant.

Substitution for $u_{rm}^{\alpha}(r)$ from Eq. (40) into Eq. (39), we get the following recurrence formula for a_k^{α} where it has been tacitly assumed that the denominator of Eq. (41a) does not vanish:

$$a_1^{\alpha} = -\frac{\beta(2t^3 + t^2 - 2t + (1-2t)m^2 - 1)}{(t+m)(t+m+2)(t-m)(t-m+2)} a_0^{\alpha}, \quad \alpha = c, s, \tag{41a}$$

$$a_k^{\alpha} = f_1 a_{k-1}^{\alpha} + f_2 a_{k-2}^{\alpha}, \quad k \geq 2, \tag{41b}$$

where

$$\begin{aligned} f_1 &= -\frac{\beta(2t^3 + m^2(3-2t-2k) + t^2(6k-5) + k(2k^2-5k+2) + 2t(3k^2-5k+1))}{f_3}, \\ f_2 &= -\frac{\beta^2(3+k^2+m^2+2k(t-2)-4t+t^2)}{f_3}, \\ f_3 &= (t+m+1+k)(t+m-1+k)(t-m+1+k)(t-m-1+k). \end{aligned} \tag{42a,b,c}$$

The exponent t in Eq. (40) is a solution of

$$(t+m+1)(t+m-1)(t-m+1)(t-m-1) = 0, \tag{43}$$

obtained by equating to zero the coefficient of a_k^{α} . It is clear that roots of the indicial Eq. (43) depend on the circumferential wave number m , and any two roots differ by an integer. The solution corresponding to the maximum root $t_{\max} = \max(t_1, t_2, t_3, t_4)$ of Eq. (43) is

$$u_{rm1}^{\alpha}(r) = \sum_{k=0}^{\infty} a_k^{\alpha} r^{k+t_{\max}}, \quad \alpha = c, s, \tag{44a}$$

and the solution for the other three roots of Eq. (43) is

$$\begin{aligned} u_{rmi}^{\alpha}(r) &= \sum_{k=0}^{\infty} \{(t-t_i) a_k^{\alpha}\}_{t=t_i} r^{k+t_i} \ln r \\ &+ \sum_{k=0}^{\infty} \{[(t-t_i) a_k^{\alpha}]_{t=t_i}\}_{t=t_i} r^{k+t_i}, \quad i = 2, 3, 4. \end{aligned} \tag{44b}$$

The complete solution for u_{rm}^{α} can be written as

$$u_{rm}^{\alpha} = \sum_{i=1}^4 C_{im}^{\alpha} u_{rmi}^{\alpha}(r), \tag{45}$$

where C_{im}^{α} is a constant.

Explicit expressions for the circumferential displacement and the hydrostatic pressure can be derived by following the same procedure as that for the power-law variation of the shear modulus.

4. Results for example problems

We first study the convergence of the Fourier series solution (8), the convergence of the Frobenius series (40), and the evaluation of the integral in Eq. (18) for a given eccentricity between the inner and the outer surfaces of the cylinder. Subsequently, we present results for several sample problems to illustrate effects of non-axisymmetric loads, the eccentricity, and the gradation of material properties. In these example problems, unless noted otherwise, we take $\mu_0 = 1$ MPa, $r_{in}/r_{ou} = 0.6$, and $r_{ou} = 1$ cm. For a few problems we compare our analytical solution with that obtained by using the commercial finite element software, ANSYS. We note that the finite element method (FEM) provides an approximate solution of a boundary-value problem whose accuracy can be improved upon by increasing the number of elements into which the problem domain is divided. While analyzing problems using ANSYS the cylinder thickness is divided into 16 uniform layers of equal thicknesses. Each layer has 400 uniform 4-node (Plane 182) elements in the circumferential direction and two elements in the radial direction. It requires solving simultaneously 39,266 algebraic equations. The value of the shear modulus in each layer is a constant and equals that obtained from Eqs. (24) or (32) at the midpoint of the layer.

In curves included in all figures, ‘a’ and ‘p’ represent, respectively, solutions obtained with the FEM and the present approach.

The number of terms in the Frobenius and the Fourier series is increased till stresses at a point have converged to within 0.1% of their values. The number of terms in these series needed to obtain a converged solution varies with the eccentricity of the cylinder and the gradation of material properties.

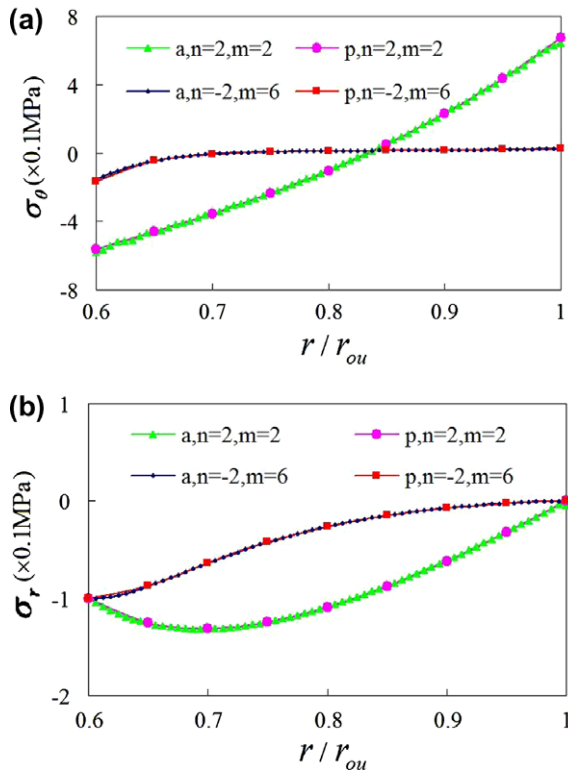


Fig. 2. Through-the-thickness distributions of (a) the hoop stress, and (b) the radial stress.

4.1. Comparison of the present solution with that from the FEM

4.1.1. Power-law variation of the shear modulus

We assume that only the inner surface of the FG hollow cylinder is loaded by pressure $p_{in} = 0.1 \times \cos(2\theta)$ MPa, $0 \leq \theta < 2\pi$, and $n = 2$ in the power-law variation (24) of the shear modulus. The problem is also analyzed for $p_{in} = 0.1 \times \cos(6\theta)$ MPa, $0 \leq \theta < 2\pi$, and $n = -2$ in Eq. (24). The analytical solutions of these two problems are obtained by retaining only the $\cos(2\theta)$ and the $\cos(6\theta)$ terms, respectively, in Eqs. (8a)–(8c). The through-the-thickness distributions of the radial and the hoop stresses computed from the two approaches are compared in Fig. 2a and b. The close agreement between solutions from the two methods suggests that for the pressure distribution expressed by a single cosine or a sine term, the analytical solution obtained easily by considering only one term in Eqs. (8a)–(8c) is close to the solution of the problem by the FEM. Furthermore, for a power-law variation of the shear modulus in the radial direction, dividing the inhomogeneous cylinder into one comprised of 16 perfectly bonded contiguous homogeneous cylinders is sufficient. In [12] problems for FG cylinders and in [25] vibrations of a FG rectangular plate have been solved by dividing the cylinder and the plate, respectively, into several layers of homogeneous materials.

4.1.2. Exponential variation of the shear modulus

We calculate stresses in an internally loaded hollow cylinder with an exponential variation in the radial direction of the shear modulus using the following parameters:

Table 1 Effect of the number of terms in the Frobenius series on stresses at the point (6.6 mm, 0).

	Number of terms in the Frobenius series						
	25	27	29	30	35	40	50
Radial stress ($\times 0.1$ MPa)	0.357805	0.359573	0.36136	0.361577	0.361534	0.361534	0.361534
Hoop stress ($\times 0.1$ MPa)	1.09346	1.16507	1.23729	1.24607	1.24434	1.24434	1.24434

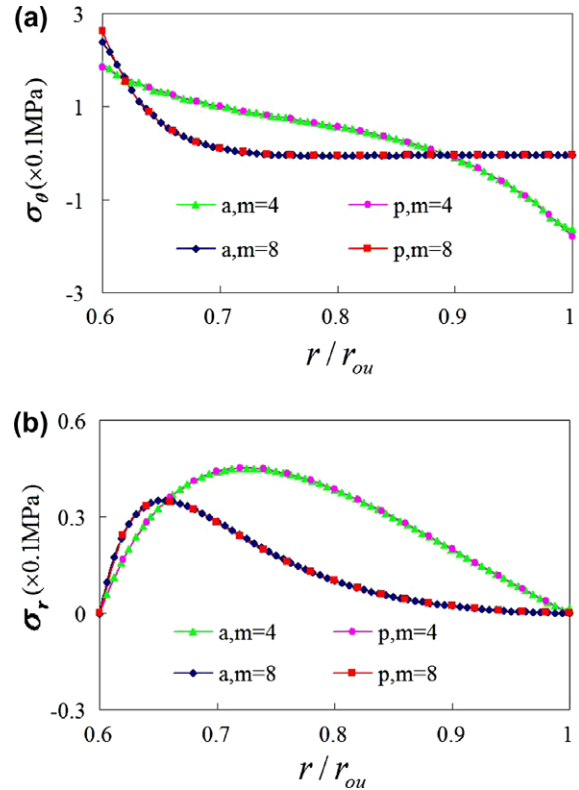


Fig. 3. Through-the-thickness distributions of (a) the hoop stress, and (b) the radial stress.

$$p_{in} = 0.1 \times \sin(4\theta) \text{ MPa}, \quad 0 \leq \theta < 2\pi, \quad \beta = 5, \quad \text{and}$$

$$p_{in} = 0.1 \times \sin(8\theta) \text{ MPa} \quad 0 \leq \theta < 2\pi, \quad \beta = -5.$$

The radial and the hoop stresses at the point (6.6 mm, 0) for different number of terms in the Frobenius series (40) when $\beta = 5$ are listed in Table 1. It is clear that with an increase in the number of terms in the Frobenius series from 30 to 50 the radial and the hoop stresses at the point (6.6 mm, 0) hardly change. It suggests that 30 terms in the Frobenius series provide a solution for which stresses at a point have converged within 0.1% of their values at that point. The through-the-thickness variations of the radial and the hoop stresses on the radial line $\theta = 0$ depicted in Fig. 3a and b and computed with the two approaches overlap each other.

4.1.3. Eccentric cylinder

We now consider two eccentric cylinders with $e/r_{ou} = 0.05$ and 0.10, the power-law variation of the shear modulus corresponding to $n = 0$ and 1, $q_{ou} = 0$, $p_{ou} = 0.1$ MPa, $0.1 \times \cos(\theta)$ MPa and $0.1 \times \cos(2\theta)$ MPa, and the inner surface of the cylinder kept fixed. The compatibility condition (7) for the solution to exist is automatically satisfied since tractions on the inner clamped boundary will be such that the overall equilibrium is maintained. The challenge is to satisfy boundary condition (5e) in the sense of Fourier series. For $p_{ou} = 0.1 \times \cos(2\theta)$ MPa and $e/r_{ou} = 0.05$, $n = 1$, we have listed in Table 2 the radial stress at the point (6.5 mm, 0) for different

Table 2

Effect of the number of Gauss integration points and the number of terms in the Fourier series on the radial stress at the point (6.5 mm, 0). Unit: 0.1 MPa.

Gauss points	Number of terms in the Fourier series									
	2	3	4	5	6	7	8	9	10	
24	-1.14266	-1.07112	-1.05021	-1.04749	-1.04722	-1.0472	-1.04719	-1.04719	-1.04719	-1.04719
32	-1.14266	-1.07112	-1.05021	-1.04749	-1.04722	-1.04719	-1.04719	-1.04719	-1.04719	-1.04719

number of terms in the Fourier series expansion of displacements and the hydrostatic pressure (cf. Eq. (8)), and the number of Gauss integration points used to numerically evaluate integrals on the left hand side of Eq. (18). It is clear that with an increase in the number of terms in the Fourier series, the radial stress at the point (6.5 mm, 0) converges. For a fixed number of terms in the Fourier series, results with 24 and 32 Gauss integration points are the same. In general, the number of terms in the Fourier series required for the solution to converge increases with an increase in the eccentricity e .

In Figs. 4 and 5 we compare the through-the-thickness distributions of the radial and the hoop stresses from the FEM and the present technique for the two eccentric cylinders. It is clear that results from the FEM and the present technique differ by less than 5%.

4.1.4. Partially loaded circular cylinder

The convergence of the Fourier series solution for the concentric cylinder with pressure applied to a part of the inner surface is also

studied. For $n = -2$, $p_{in}(\theta) = 0.1$ MPa, $-\pi/2 \leq \theta \leq \pi/2$ and the outer surface fixed, stresses at the point $(r_{in}, 0)$ are listed in Table 3. It is evident that the radial and the hoop stresses at the point $(r_{in}, 0)$ converge with an increase in the number of terms in the Fourier series, and 35 terms in the Fourier series solution should suffice. Even though magnitudes of stresses oscillate the amplitude of oscillations is less than 2% of the magnitude of the stress. We note that the magnitude of the hoop stress is less than that of the radial stress, and the number of terms needed to get converged values of stresses is four times that for the case of the uniform pressure applied on the inner surface of a hollow cylinder.

4.2. Parametric studies

We have conducted parametric studies to illuminate effects of (i) the gradation of material properties, (ii) the circumferential wave number of the pressure applied on the inner surface of a hollow cylinder, (iii) the pressure applied only on a part of the inner surface of a cylinder, (iv) tangential tractions applied on the inner surface, and (v) the eccentricity of the cylinder. We also give results for a thin cylinder with a non-axisymmetric pressure applied

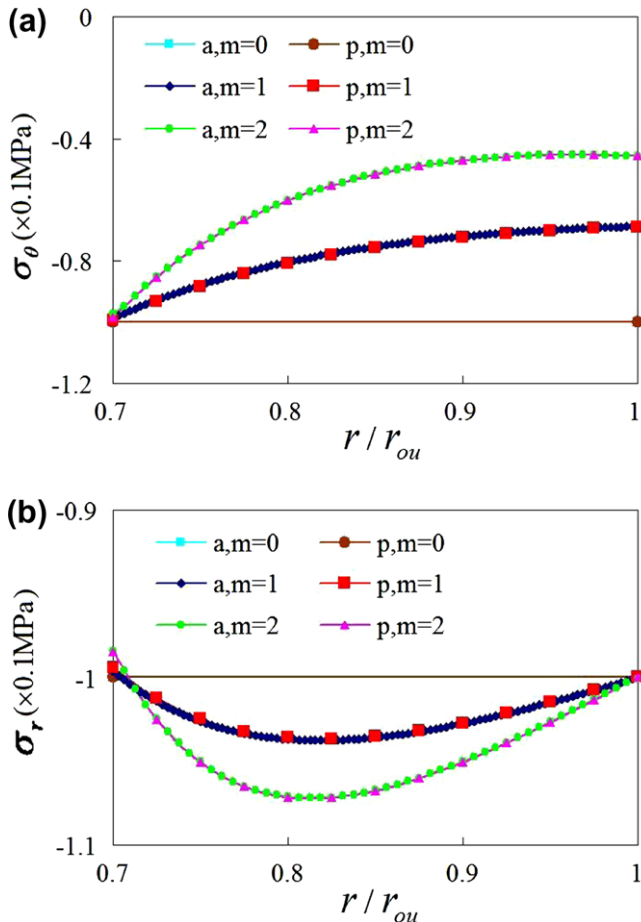


Fig. 4. For eccentric cylinders made of a homogeneous material having $e/r_{ou} = 0.1$ and three different pressure distributions (corresponding to $m = 0, 1$ and 2) on the outer surface, comparison from the two solution techniques of through-the-thickness distributions of (a) the hoop stress, and (b) the radial stress.

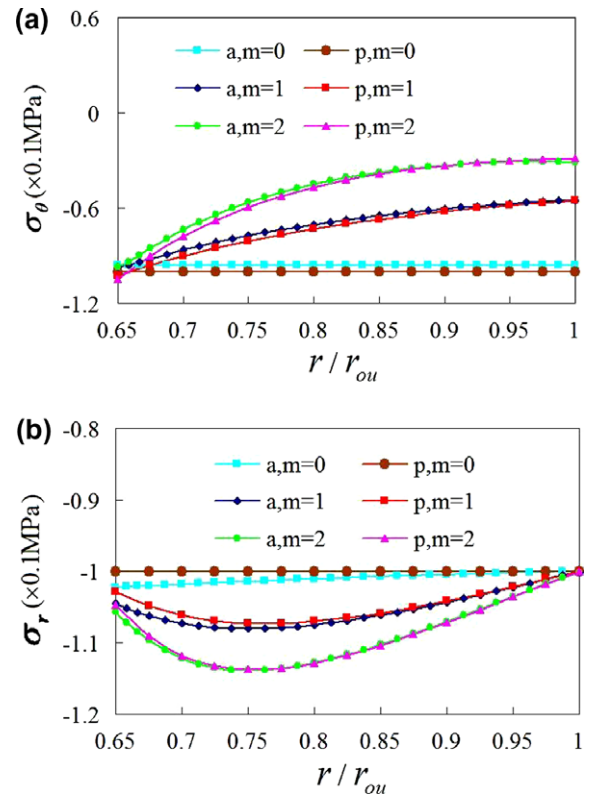


Fig. 5. For an eccentric cylinder with the shear modulus a linear function of the radius, $e/r_{ou} = 0.05$, and three different pressure distributions (corresponding to $m = 0, 1$ and 2) on the outer surface, comparison from the two solution techniques of through-the-thickness distributions of (a) the hoop stress, and (b) the radial stress.

Table 3
Radial and hoop stresses at the point $(r_{in}, 0)$ for different number of terms in the Fourier series.

	Number of terms in the Fourier series							
	35	37	39	41	43	45	47	49
Radial stress ($\times 0.1$ MPa)	-0.991165	-1.00837	-0.992047	-1.00757	-0.992769	-1.00692	-0.993371	-1.00636
Hoop stress ($\times 0.1$ MPa)	-0.729089	-0.747276	-0.730072	-0.746394	-0.730868	-0.745672	-0.731525	-0.74507

on its inner surface, and for a very thick cylinder with a non-axisymmetric pressure applied on the outer surface.

4.2.1. Hollow cylinder with non-axisymmetric surface tractions

4.2.1.1. Gradation of material properties. For $p_{in}(\theta) = 0.1 \times \cos(2\theta)$ MPa, $0 \leq \theta < 2\pi$, $p_{ou} = 0$, and the exponent $n = -2, -1, 0, 1, 2$ in Eq. (24) representing the power-law variation of the shear

modulus, we have plotted in Fig. 6a–f on the radial line $\theta = 0$ the through-the-thickness variations of the radial and the hoop stresses, the radial and the circumferential displacements, and the shear stress. The value of a quantity at a point (r, θ) is obtained by multiplying the value plotted for r by $\cos(2\theta)$. For comparison purposes results are also included for the uniform pressure 0.1 applied on the inner surface of a FG cylinder with

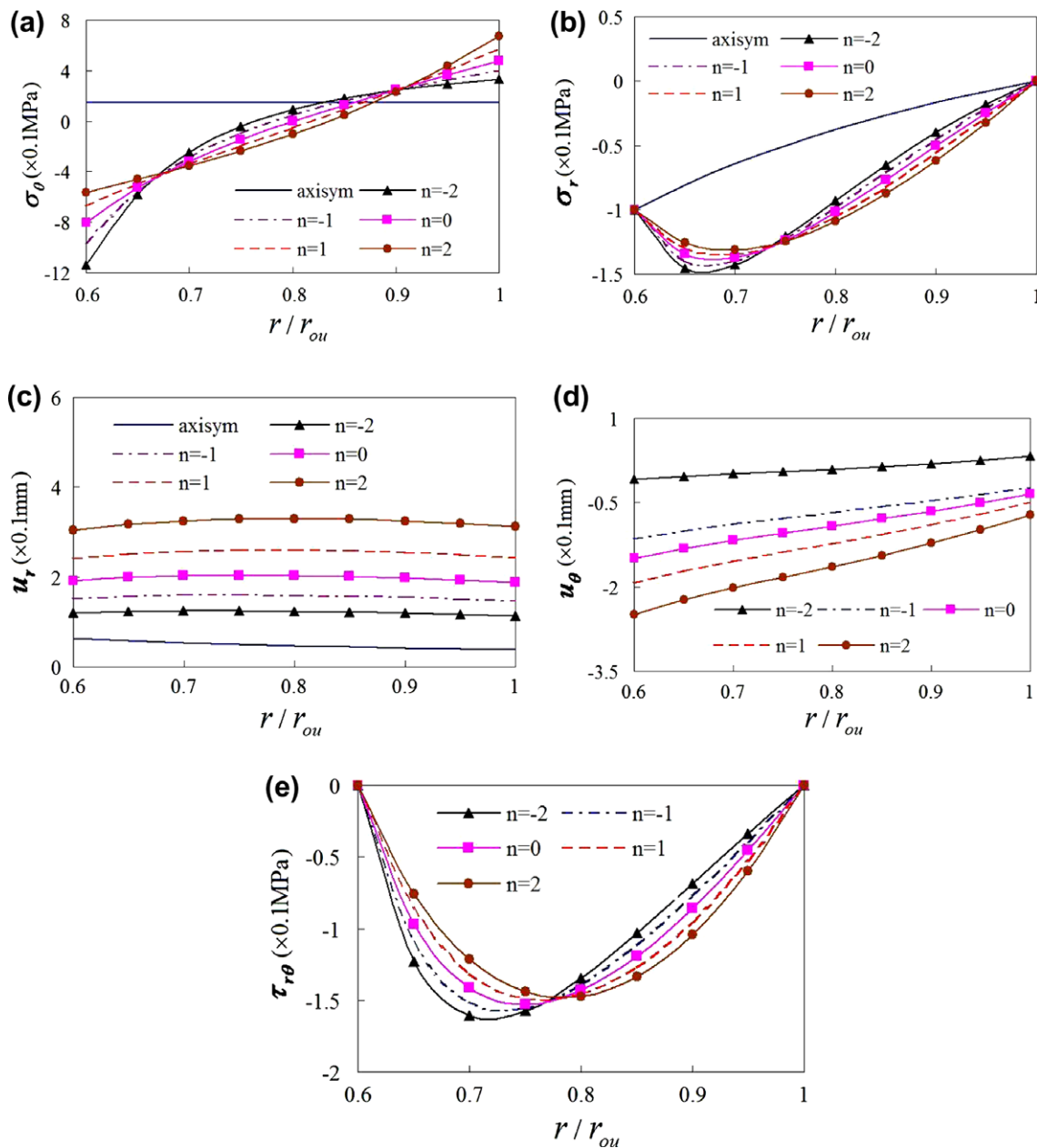


Fig. 6. For power-law variation of the shear modulus with exponent $n = -2, -1, 0, 1$ and 2 , through-the-thickness distributions of (a) the hoop stress, (b) the radial stress, (c) the radial displacement, (d) the circumferential displacement on the radial line $\theta = 0$, and (e) the shear stress on the radial line $\theta = \pi/4$. Results for an axisymmetric problem in the FG cylinder with the power law exponent $n = 1$ are also shown; the shear stress for the axisymmetric problem identically vanishes.

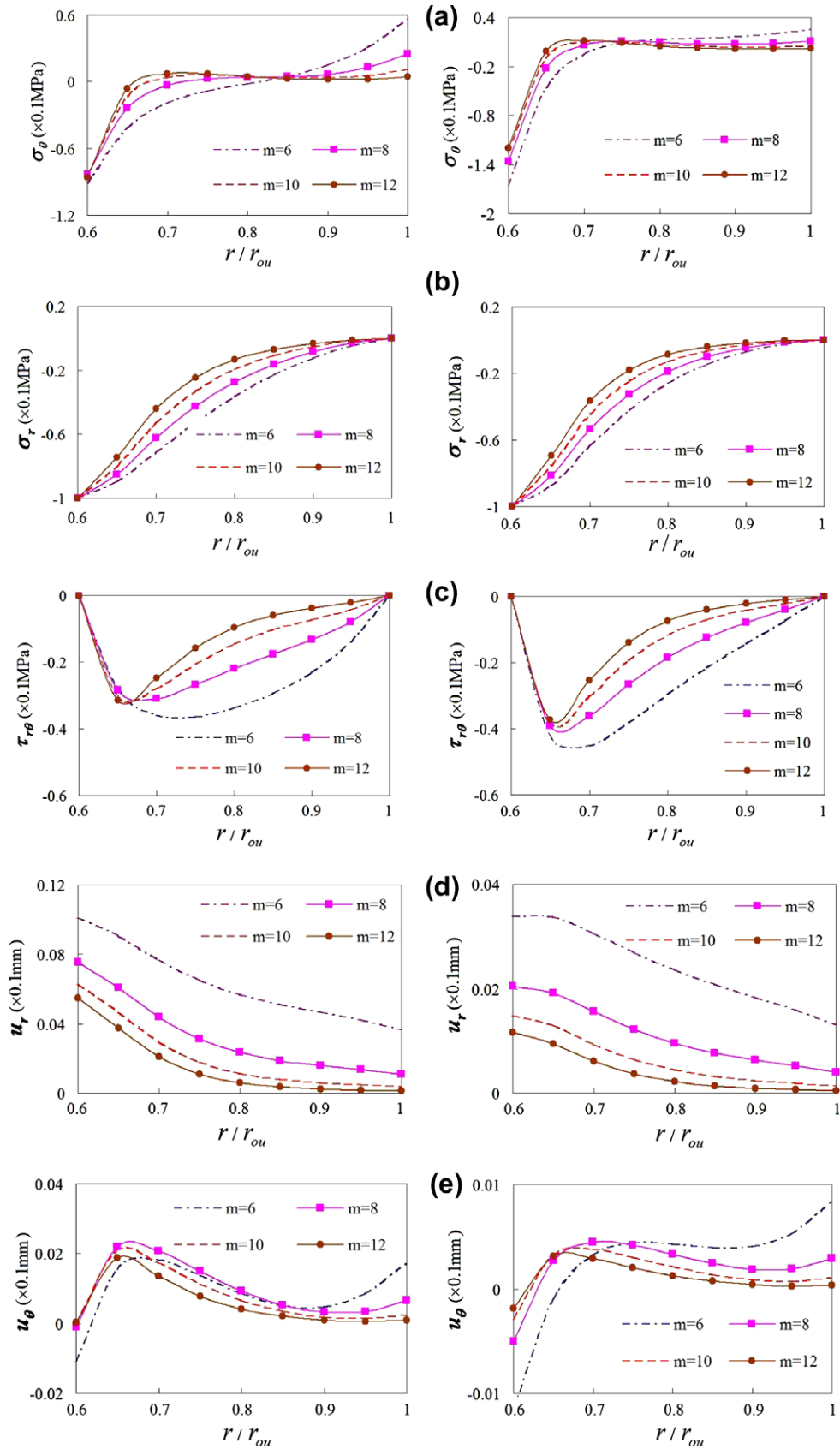


Fig. 7. For power-law variation of the shear modulus with exponent $n = 2$ (left figures) and -2 (right figures), and non-axisymmetric pressure $0.1\cos(m\theta)$ on the inner surface, through-the-thickness distributions of (a) the hoop stress, (b) the radial stress, (c) the shear stress, (d) the radial displacement, and (e) the circumferential displacement.

$n = 1$. For this axisymmetric problem, Batra [14] proved analytically that the hoop stress is a constant through the cylinder

thickness. Results for this problem are labeled ‘axisym’ in Fig. 6a–f.

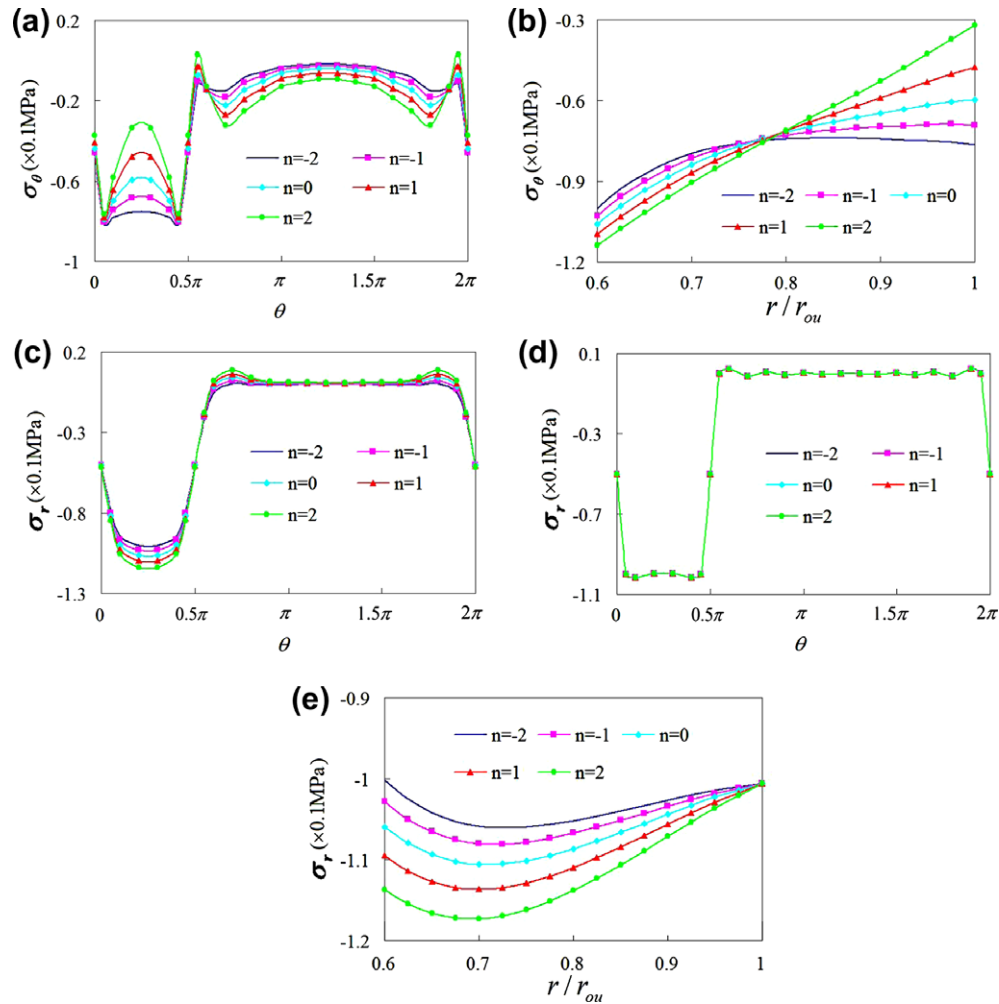


Fig. 8. For uniform pressure applied only on a quarter of the outer surface, distributions of the hoop stress on (a) the surface $r = r_{ou}$, (b) the radial line $\theta = \pi/4$, and distributions of the radial stress on (c) the surface $r = r_{in}$, (d) the surface $r = r_{ou}$, and (e) the radial line $\theta = \pi/4$.

Results presented in Fig. 6 reveal that displacements and stresses depend continuously upon the exponent n since in varying n from -2 to 2 the value of each one of these quantities changes gradually. Whereas under a uniform pressure applied to the inner surface of a homogeneous cylinder (i.e. $n = 0$) the hoop stress is tensile, for a non-uniform pressure distribution it can be compressive and of rather large magnitude. Furthermore, the hoop stress under a non-uniform pressure applied to the inner surface of the cylinder varies from large negative values at points on the inner surface of the cylinder to positive values at points on the outer unloaded surface of the cylinder. The maximum value of the radial stress does not occur at points on the inner surface of the cylinder as it does for a homogeneous cylinder but at an interior point. For each one of the five values of n and the cylinder geometry considered here, the maximum magnitude of the radial stress exceeds that of p_{in} and the location of this point moves slightly inwards with an increase in the value of n from -2 to 2 . At $r/r_{ou} \approx 0.75$, the magnitude of the radial stress is independent of the value of n ; there are two interior points where the magnitude of the hoop stress is nearly independent of the value of n . The maximum magnitude of each one of the radial, the hoop and the shear stress decreases gradually as n is increased from -2 to 2 , and these do not occur at the same interior point. At an interior point, with an increase in the value of n from -2 to 2 , magnitudes of the radial and the circumferential displacements increase.

For the exponent $n = 2$ and -2 in Eq. (24) we scrutinize deformations of the thick cylinder for

$$p_{in}(\theta) = 0.1 \times \cos(m\theta) \text{ MPa}, \quad 0 \leq \theta < 2\pi, \quad m = 6, 8, 10, 12.$$

For the four distributions of the pressure on the inner surface, stresses and displacements in the cylinder calculated using the present formulation are shown in Fig. 7. For $n = 2$, the influence of the non-axisymmetric pressure applied to the inner surface of the cylinder on the hoop stress spreads gradually along a radial line, but for $n = -2$, it is concentrated mostly at points in the vicinity of the inner surface of the cylinder. The shear stress and the two displacements at a point are affected more by the circumferential wave number m of the prescribed pressure than the hoop stress except for the increase in m from 6 to 8. Thus a small value of m seems to have a large effect on the through-the-thickness variation of a deformation variable than a large value of m . For $n = 2$ magnitudes of the radial and the tangential displacements at a point are greater than those for $n = -2$. Thus by suitably tailoring the variation in the thickness direction of the shear modulus, one can control displacements and stresses in the cylinder even when the pressure on the inner surface is not uniform.

4.2.1.2. Uniform pressure applied on a quarter of the outer surface. For the uniform pressure $p_{ou}(\theta) = 0.1 \text{ MPa}$, $0 \leq \theta \leq \pi/2$ applied to a quarter of the outer surface, the inner surface of the cylinder kept

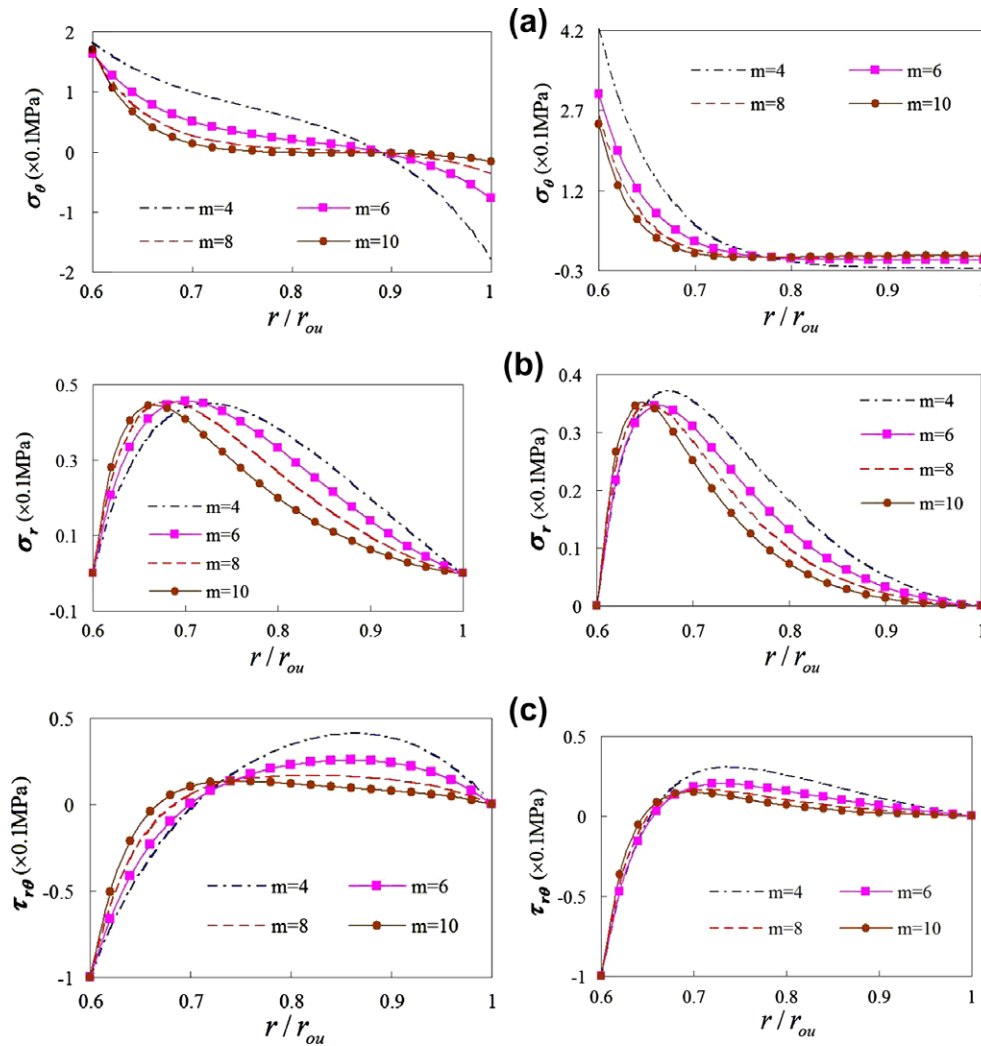


Fig. 9. For exponential variation of the shear modulus with $\beta = 5$ (left figures) and $\beta = -5$ (right figures), and the tangential traction $0.1\sin(m\theta)$ MPa applied on the inner surface, through-the-thickness distributions of (a) the hoop stress, (b) the radial stress, and (c) the shear stress.

fixed, and the exponent $n = -2, -1, 0, 1, 2$ in Eq. (24) for the power-law variation of the shear modulus, results computed with fifty terms in the Fourier series are exhibited in Fig. 8. Results for the five values of the exponent n in Eq. (24) are qualitatively similar to each other. Both the radial stress on the inner fixed surface and the hoop stress on the outer periphery decay rapidly with θ as one moves away from extremities of the loaded region. The through-the-thickness distributions for $0 < \theta < \pi/2$ are essentially similar to that for a cylinder with uniform pressure applied to its outer boundary.

4.2.1.3. Non-axisymmetric tangential tractions applied on the inner surface. We analyze deformations of a hollow cylinder with the outer surface traction free, tangential traction $q_{in}(\theta) = 0.1 \times \sin(m\theta)$ MPa, $0 \leq \theta < 2\pi$, $m = 4, 6, 8, 10$ acting on the inner surface, and the exponential variation of the shear modulus in the radial direction given by $\mu_0 \exp[-5(r - r_{in})]$, $\mu_0 \exp[5(r - r_{ou})]$. For non-zero even values of m , the compatibility condition (7) is satisfied by the prescribed tangential tractions; otherwise balancing tangential tractions need to be applied on the outer surface of the cylinder. The solution, found by retaining thirty terms in the Frobenius series, is depicted in Fig. 9. Stress distributions for the four values of m agree qualitatively suggesting that the circumferential wave number of the tangential tractions prescribed on the

inner surface does not affect the stress distribution noticeably. However, results for $m = 4$ are quantitatively different from those for the other three values of m . Distributions of the radial and the shear stresses for $\beta = -5$ and $\beta = 5$ are qualitatively similar to each other, but the two distributions of the hoop stress differ noticeably. For $\beta = 5$ and $\beta = 5$, the hoop stress varies from $+0.18$ MPa at points on the inner surface to -0.18 MPa at points on the outer surface; however, for $\beta = -5$, it varies smoothly from 0.42 MPa at points on the inner surface to -0.03 MPa at points on the outer surface. For $\beta = -5$ and for each one of the four values of m , the hoop stress drops rather rapidly from its maximum value at points on the inner surface to -0.03 MPa at $r/r_{ou} = 0.75$; the rate of drop is a little less for the circumferential wave number $m = 4$ than that for the other three values of m . Whereas the maximum value of the hoop stress occurs at a point on the inner surface that of the radial and the shear stresses occurs at interior points whose locations vary with the value of m . The maximum hoop stress is greater than the maximum magnitude of the shear stress. These results suggest that for a FG cylinder with the shear modulus decreasing with an increase in r , large values of stresses occur within one-third the cylinder thickness from the inner surface. However, when the shear modulus increases with an increase in r , the magnitude of the hoop stress for $m = 4$ at points on the outer surface is comparable to that at points on the inner surface.

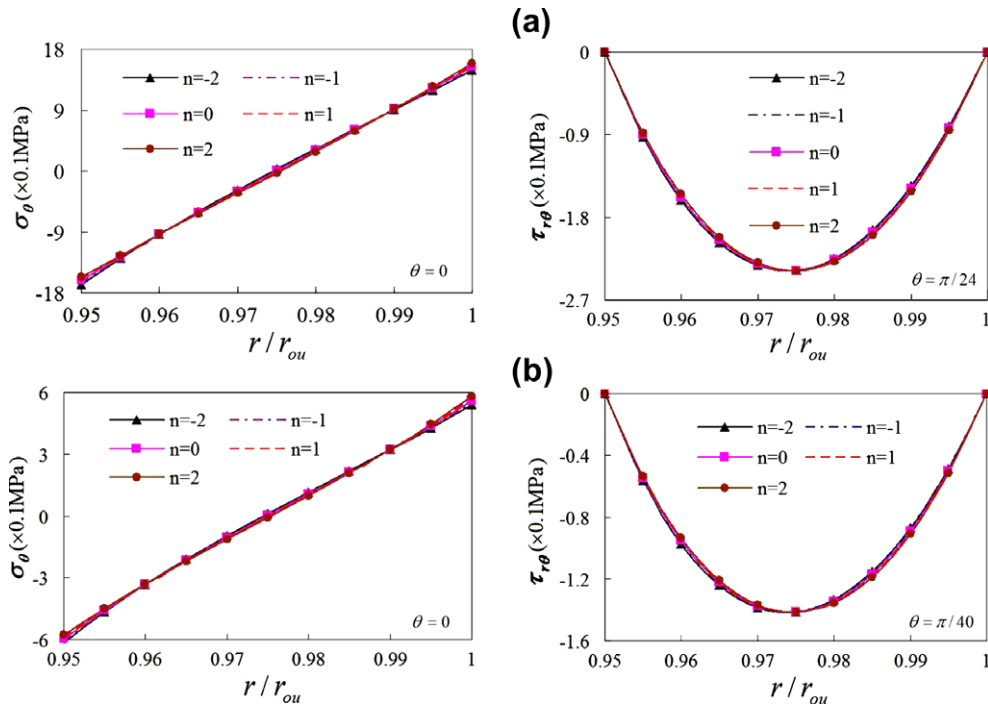


Fig. 10. For (a) $m = 12$ (top) and (b) $m = 20$ (bottom), $r_{in}/r_{ou} = 0.95$, through-the-thickness distributions of the hoop and the shear stresses.

4.2.1.4. *Non-axisymmetric pressure applied to a thin cylinder.* For $r_{in}/r_{ou} = 0.95$, $p_{in} = 0.1 \times \cos(m\theta)$ MPa, $0 \leq \theta < 2\pi$, $p_{ou} = 0$, $m = 12, 20$ and the exponent $n = -2, -1, 0, 1$ and 2 , we have plotted in Fig. 10 on a radial line through-the-thickness variations of the hoop stress and the shear stress to delineate effects of the non-axisymmetric pressure distribution on the surface tension and the shear stresses induced in the thin cylinder. These results show that the maximum hoop stress and the maximum shear stress strongly depend upon the circumferential wave number of the applied pressure. With an increase in the circumferential wave number from 12 to 20, the maximum hoop stress decreases from 1.6 to 0.6 MPa and the maximum shear stress from 0.23 to 0.14 MPa. We note that these stress distributions are nearly independent of the gradation of material properties. The variation of σ_θ from negative values on the inner surface to positive values on the outer surface of the same magnitude suggests that bending rather than stretching deformation are dominant in each one of the angular segments of length $2\pi/m$. For a uniformly loaded simply supported beam, the maximum axial stress is proportional to the square of the beam length. Thus for pure bending of the segment of thin cylinder between two cusps of the applied pressure, the maximum hoop stress for $m = 20$ should be 36% of that for $m = 12$ which is not too different from the 37.5% obtained here. Recall that for a uniform pressure distribution corresponding to $m = 0$, the shear stress vanishes identically, the hoop stress is almost constant and equals nearly twenty times the uniform pressure, and the cylinder wall deforms due to stretching rather than due to bending deformations.

4.2.1.5. *Non-axisymmetric pressure applied to the outer surface of a very thick cylinder.* We have analyzed deformation of a very thick

cylinder with $r_{ou} \gg r_{in}$, $p_{ou} = 0.1 \times \cos(m\theta)$ MPa, $0 \leq \theta < 2\pi$, $m = 0, 2, 6, 12$, $p_{in} = 0$ and the exponent $n = -2, 0$ and 2 . For $n = -2, 0, 2$ and $m = 0$ and 2 , the maximum hoop stress occurs at the tiny hole, and the values are listed in Table 4. We note that for $m = n = 0$, the maximum hoop stress of 0.2 MPa listed in Table 4 agrees with that given in [14]. As should be clear from the values listed in Table 4, the maximum hoop stress at the surface of a tiny hole strongly depends upon the values of n and m . For $n = -2$, the maximum hoop stress at the hole for $m = 2$ is about 3.5 times that for $m = 0$. However, the maximum hoop stress at the hole is significantly reduced when n is changed from 0 to 2. Thus the gradation in the radial direction of the shear modulus significantly affects the maximum hoop stress induced at the surface of a hole in a thick cylinder. For $n = -2, 0, 2$, the hoop stress at the hole surface changes from compressive for $m = 0$ to tensile for $m = 2$. For $n = -2$ and 2 , and the four values of m , the through-the-thickness variations of σ_{rr} and $\sigma_{\theta\theta}$ are plotted in Fig. 11. These plots evince that for $m = 6$ and 12 stresses, except at points near the outer surface, are nearly uniform through the cylinder thickness.

4.2.2. *Eccentric cylinder*

4.2.2.1. *Gradation of material properties.* For an eccentric cylinder with $e/r_{ou} = 0.05$, the exponent n in the power law relation (24) equal to $-2, -1, 0, 1$ and 2 , the inner surface of the cylinder fixed and the pressure $p_{ou} = 0.1 \times \cos(2\theta)$ MPa, $0 \leq \theta < 2\pi$ applied to the outer surface, Fig. 12 exhibits through-the-thickness variations of the hoop and the radial stresses. Results have been computed by retaining eight terms in the Fourier series and using 24 Gauss points to numerically evaluate integrals in Eq. (18). For each value of n , the through-the-thickness distributions of the hoop and the radial stresses on the radial line where the cylinder thickness is

Table 4
Hoop stress at a tiny hole in a very thick cylinder. Unit: 0.1 MPa.

	$r_{in}/r_{ou} = 0.1$			$r_{in}/r_{ou} = 0.05$			$r_{in}/r_{ou} = 0.025$		
	$n = -2$	$n = 0$	$n = 2$	$n = -2$	$n = 0$	$n = 2$	$n = -2$	$n = 0$	$n = 2$
$m = 0$	-4.0004	-2.0202	-0.4343	-4.0000	-2.0050	-0.3338	-4.0000	-2.0013	-0.2710
$m = 2$	12.6087	4.1220	0.2492	13.2928	4.03013	0.0675	13.6919	4.0075	0.0176

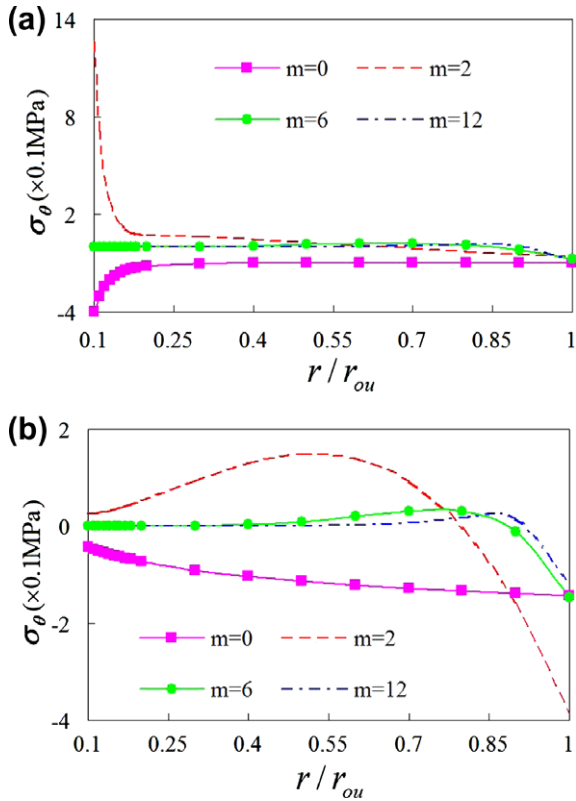


Fig. 11. For $r_{in}/r_{ou} = 0.1$, and four values of the circumferential wave number of the pressure applied to the outer surface through-the-thickness distributions of the maximum hoop stress; (a) $n = -2$, and (b) $n = 2$.

the maximum are similar to those on the radial line where the cylinder thickness is the minimum. However, the influence of the eccentricity on the stresses in the cylinder with the exponent $n = 2$ is greater than that in the cylinder with the exponent $n = -2$. The magnitudes of the radial stress at interior points vary

between 0.1 and 0.13 MPa irrespective of the value of n and where the point is located.

4.2.2.2. Eccentricity of the cylinder. For an eccentric cylinder with $e/r_{ou} = 0.05, 0.10, 0.15$ and 0.20 , the exponent n in the power law relation (24) equal to -2 and 2 , the inner surface of the cylinder fixed and the pressure $p_{ou} = 0.1 \times \cos(2\theta)$ MPa, $0 \leq \theta < 2\pi$ applied to the outer surface, variations of stresses in the circumferential and the radial directions are exhibited in Figs. 13 and 14. Results are computed by retaining thirty terms in the Fourier series and using 128 Gauss points to evaluate integrals in Eq. (18). These results evince that the eccentricity does not significantly change the magnitude of stresses on the inner surface of the cylinder, and the stress distribution has the same circumferential wave number as the applied pressure. Furthermore, stresses depend continuously upon the eccentricity. For the largest value $e/r_{ou} = 0.2$ of the eccentricity considered, the hoop stress on the inner surface in the neighborhood of the point $\theta = \pi$ varies smoothly for $n = 2$ but not so smoothly for $n = -2$. Also, the radial and the hoop stresses at a point do not equal principal stresses there because of non-zero shear stress. At interior points on the radial lines $\theta = \pi$ and $\theta = 0$ the maximum magnitude of the hoop stress occurs at a point on the inner surface. The maximum magnitude of the radial stress exceeds that of the external pressure and the point where it occurs varies with the eccentricity of the cylinder. For $n = 2$ and -2 the shear stress at a point varies smoothly with the change in the eccentricity.

The distributions on the inner fixed surface of principal stresses for the cylinders with $e = 0$ and $e/r_{ou} = 0.2$ are exhibited in Fig. 15. As mentioned above, the principal stresses at a point need not equal the hoop stress and the radial stress since the shear stress $\sigma_{r\theta}$ may not vanish. However, one of the principal stresses equals the hydrostatic pressure since $\sigma_{z\theta}$ and σ_{rz} equal zero. Since the three principal stresses have nearly the same magnitude, the hydrostatic pressure significantly contributes to the other two principal stresses, and to the radial and the hoop stresses. Both the eccentricity and the exponent n in the power law relation (24) noticeably affect the variation with θ of the principal stresses. For the cylinder with zero eccentricity, stress distributions on the

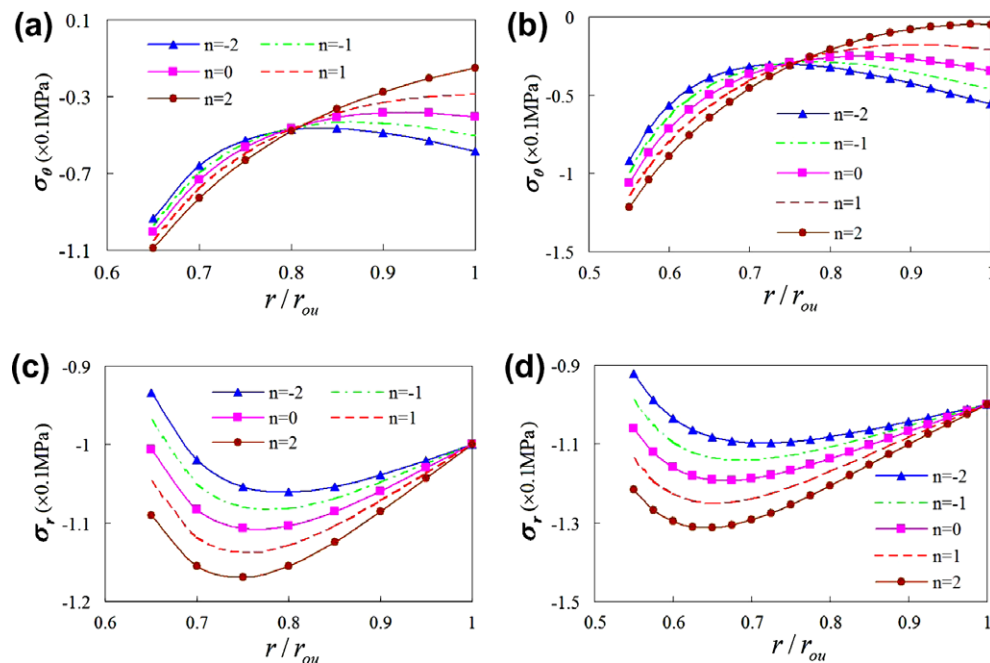


Fig. 12. For $e/r_{ou} = 0.05$, through-the-thickness distributions of (a) the hoop stress on the line $\theta = 0$ (the minimum thickness), (b) the hoop stress on the line $\theta = \pi$ (the maximum thickness), (c) the radial stress on the line $\theta = 0$ (the minimum thickness), and (d) the radial stress on the line $\theta = \pi$ (the maximum thickness).

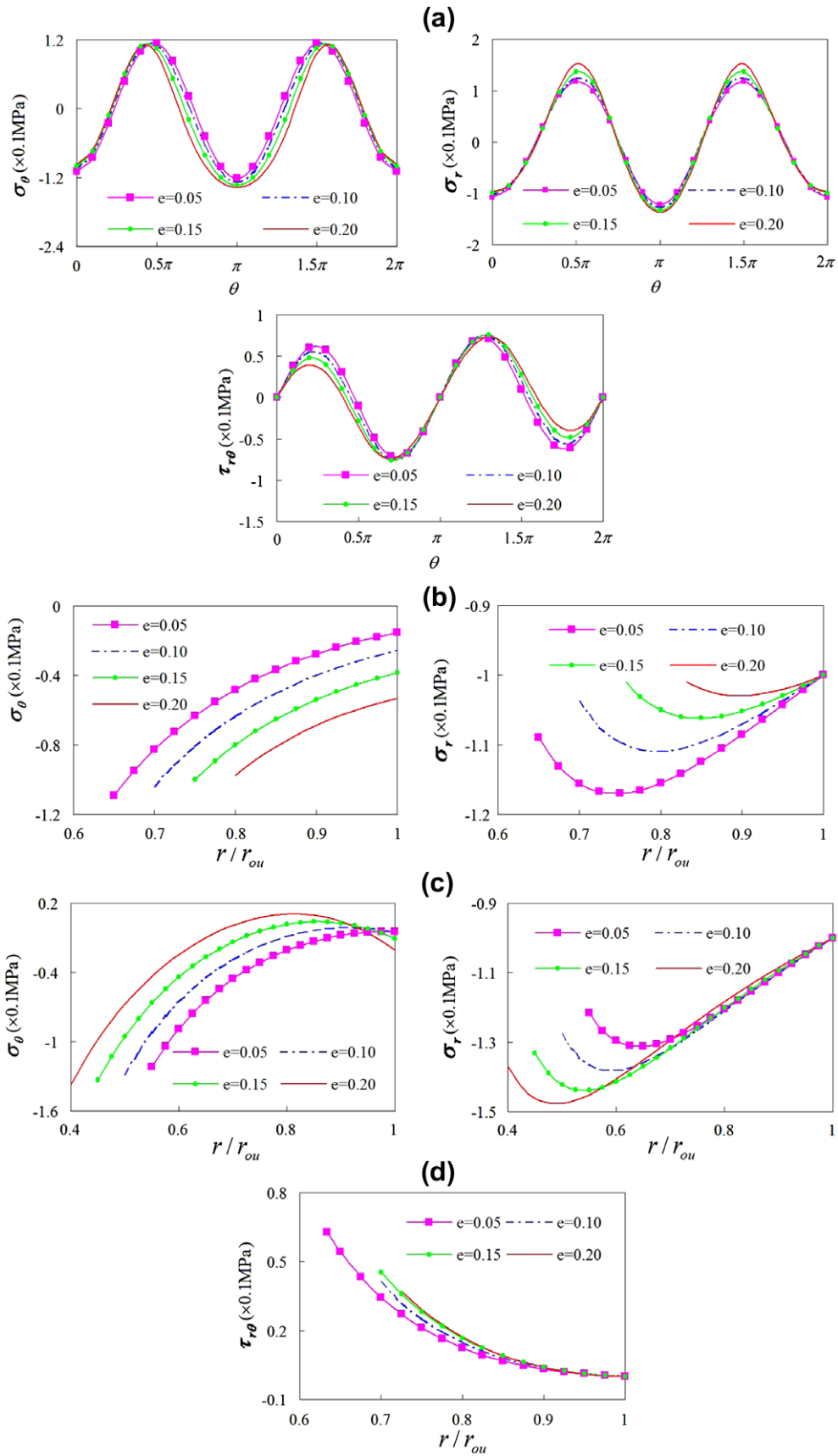


Fig. 13. For four values of the eccentricity e , and the exponent $n = 2$ in Eq. (24), distributions of stresses on the (a) inner surface, $r = r_{in}$, (b) the radial line $\theta = 0$ (the minimum thickness), (c) the radial line $\theta = \pi$ (the maximum thickness), and (d) the shear stress on the radial line $\theta = \pi/4$.

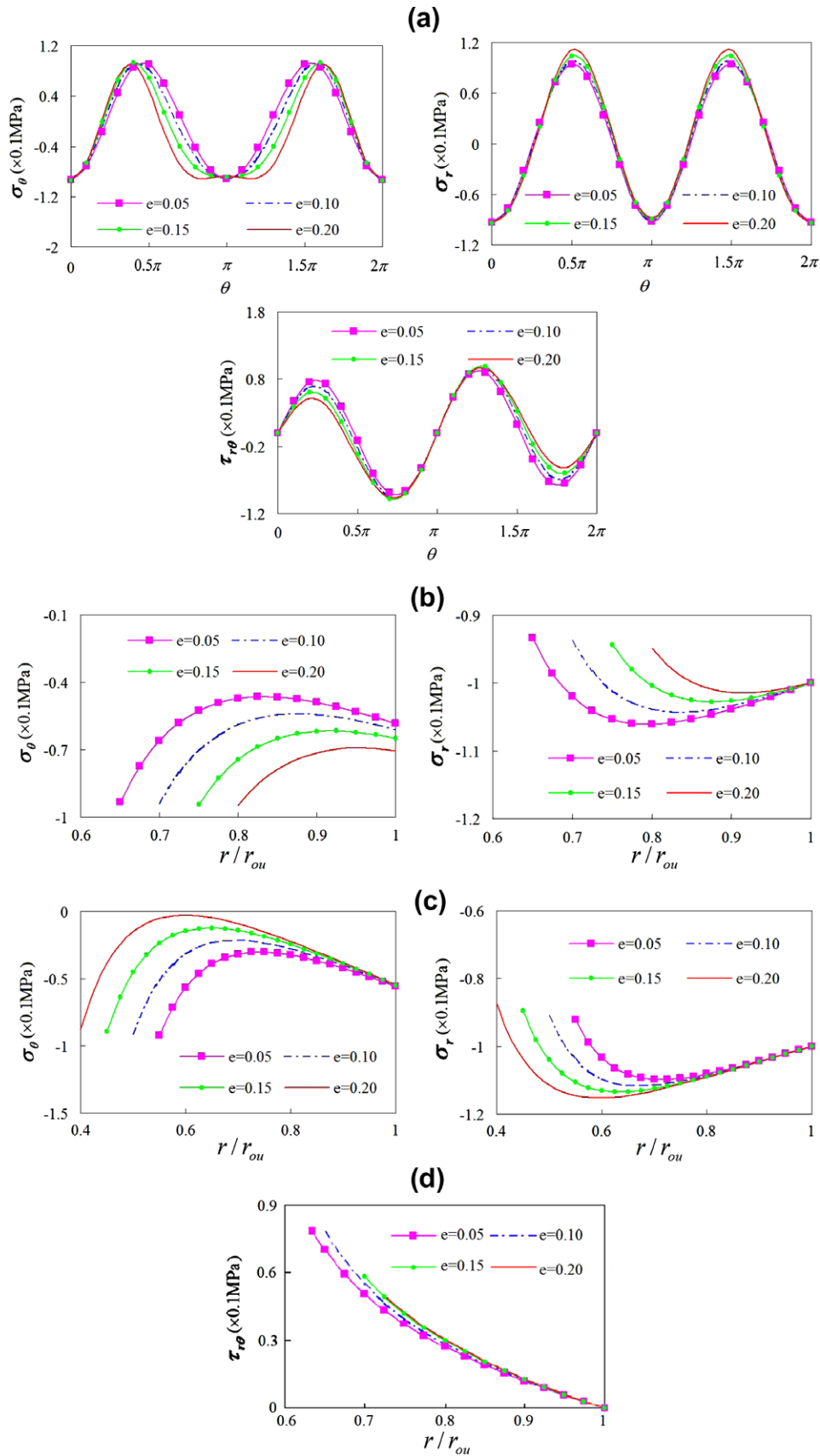


Fig. 14. For four values of the eccentricity e , and the exponent $n = -2$ in Eq. (24), distributions of stresses on the (a) inner surface, $r = r_{in}$, (b) the radial line $\theta = 0$ (the minimum thickness), (c) the radial line $\theta = \pi$ (the maximum thickness), and (d) the shear stress on the radial line $\theta = \pi/4$.

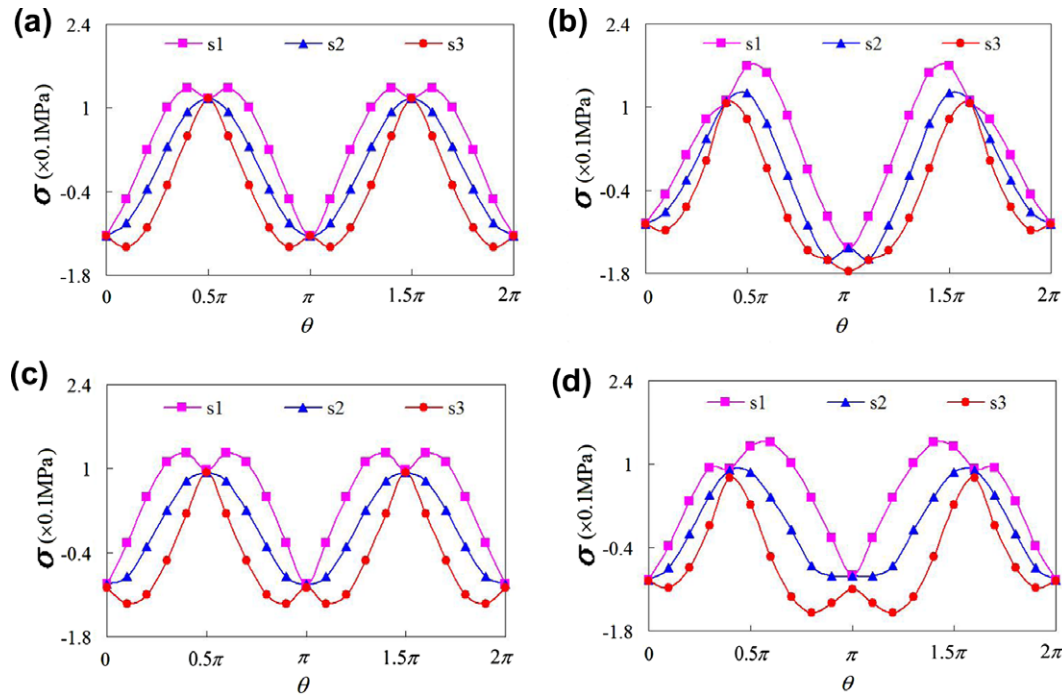


Fig. 15. Variations of principal stresses on the fixed inner surface of the cylinder for (a) $n = 2, e/r_{ou} = 0.0$, (b) $n = 2, e/r_{ou} = 0.2$, (c) $n = -2, e/r_{ou} = 0$, and (d) $n = -2, e/r_{ou} = 0.2$.

inner fixed surface are virtually unaffected when n in Eq. (24) is changed from -2 to 2 . However, for an eccentric cylinder, the change in n from -2 to 2 has a noticeable effect on the stress distribution on the fixed surface. For the cylinder with zero eccentricity the maximum principal stress of 0.13 MPa occurs at $\theta = 0.4\pi$ and for the eccentric cylinder the maximum principal stress equals 0.17 MPa for $n = 2$ at the point $\theta = 0.5\pi$ and equals 0.14 MPa for $n = -2$ at the point $\theta = 0.6\pi$.

From values of the maximum principal stress versus the eccentricity plotted in Fig. 16 it is clear that for $n = 2$ the maximum principal stress induced in the cylinder increases monotonically with an increase in e but for $n = -2$ it seems to saturate at $e/r_{ou} = 0.1$ and barely increases when the eccentricity is doubled. Thus the effect of eccentricity on the maximum principal stress induced in the cylinder can be mitigated by tailoring the gradation of the shear modulus through the cylinder thickness.

5. Remarks

For a FG cylinder comprised of two or more materials one can use an homogenization technique (e.g. the rule of mixture, the 3-phase rule, the equivalent energy principle; see [21] and references

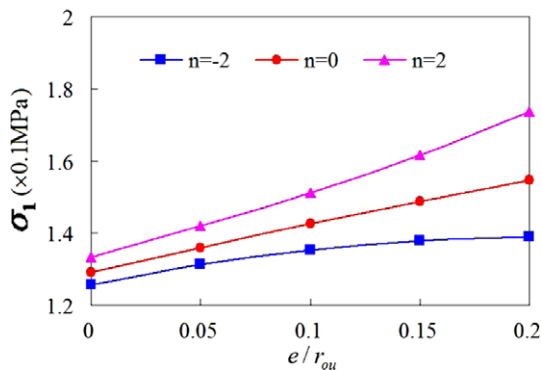


Fig. 16. Variation with the eccentricity of the maximum principal stress.

cited therein) to ascertain volume fractions of constituents needed to obtain the desired gradation of the shear modulus in the radial direction. The material tailoring problem, i.e., finding the gradation of material properties so as to achieve a desired state of stress within the body has been discussed in [22–24].

6. Conclusions

We have analyzed analytically plane strain infinitesimal deformations of a non-axisymmetrically loaded hollow cylinder and of an eccentric cylinder composed of a linear elastic isotropic and incompressible functionally graded (FG) material. The shear modulus in the radial direction is assumed to vary either according to a power law relation or an exponential function. The convergence of the infinite series in the analytical solution has been established, and solutions for a few problems are found to compare very well with their solutions obtained by the finite element method using a commercial computer code with the cylinder divided into sixteen contiguous perfectly bonded homogeneous cylinders. The shear modulus of each one of the sixteen cylinders equals that of the functionally graded cylinder evaluated at the mean radius of the layer. We have delineated effects of the eccentricity and of the gradation of the shear modulus upon deformations of a cylinder.

It is found that for a hollow FG cylinder with uniform pressure applied to the inner surface only, the maximum value of the radial stress does not occur at points on the inner surface of the cylinder as it does for a homogeneous cylinder but at an interior point. The hoop stress in the cylinder can be compressive and of rather large magnitude under a non-uniform pressure. For a hollow cylinder with non-axisymmetric tangential traction acting on the inner surface, the maximum hoop stress is greater than the maximum magnitude of the shear stress. The maximum value of the hoop stress occurs at a point on the inner surface and that of the radial and the shear stresses occurs at interior points whose locations vary with the circumferential wave number of the load.

The maximum hoop and shear stresses in a thin cylinder strongly depend upon the circumferential wave number of the applied non-axisymmetric pressure. For large circumferential wave

number of the applied pressure, bending rather than stretching deformations of the cylinder segment between two cusps of the applied pressure are dominant.

For a very thick FG cylinder with pressure applied only on the outer surface, the magnitude and the sign of the hoop stress on the inner surface strongly depend upon the gradation of material properties and on the circumferential wave number of the applied load.

The maximum principal stress in a FG eccentric cylinder can be controlled by suitably varying the shear modulus in the radial direction.

Acknowledgments

This work was partially supported by the Office of Naval Research Grant N00014-98-06-1-0567 to Virginia Polytechnic Institute and State University with Dr. Y.D.S. Rajapakse as the program manager. Views expressed herein are those of authors, and neither of the funding agencies nor of their institutions.

Appendix A

Expressions for f_{ri}, f_{oi}, f_{pi} ($i = 1, 2, 3$)

$$f_{r1} = \frac{2}{\beta r} + \frac{\ln r}{2} - \frac{3}{2\beta^2 r^2},$$

$$f_{r2} = \frac{3 \exp(-\beta r)}{4\beta^6 r^2} - \frac{\exp(-\beta r)}{4\beta^5 r} - \frac{\text{Ei}(-\beta r)}{4\beta^4},$$

$$f_{r3} = -\frac{13}{16\beta^2} + \frac{5\gamma}{8\beta^2} + \frac{15 \exp(-\beta r)}{8\beta^4 r^2} - \frac{11 \exp(-\beta r)}{8\beta^3 r} - \frac{3\text{Ei}(-\beta r)}{4\beta^2} - \frac{3\text{Ei}(-\beta r)}{4\beta^4 r^2} + \frac{\text{Ei}(-\beta r)}{\beta^3 r} + \frac{5\Gamma(0, \beta r)}{8\beta^2} - \frac{(r_p)F_q[\{1, 1, 1\}; \{2, 2, 2\}; -\beta r]}{2\beta} - \frac{5 \ln(r)}{8\beta^2} + \frac{\gamma \ln(r)}{2\beta^2} + \frac{3 \exp(-\beta r) \ln(r)}{4\beta^4 r^2} - \frac{\exp(-\beta r) \ln(r)}{4\beta^3 r} + \frac{\text{Ei}(-\beta r) \ln(r)}{4\beta^2} + \frac{\Gamma(0, \beta r) \ln(r)}{2\beta^2} - \frac{\ln^2(r)}{4\beta^2} + \frac{5 \ln(\beta r)}{8\beta^2} + \frac{\ln(r) \ln(\beta r)}{2\beta^2},$$

$$f_{o1} = -\frac{1}{2} - \frac{3}{2\beta^2 r^2} - \frac{\ln(r)}{2},$$

$$f_{o2} = \frac{3 \exp(-\beta r)}{4\beta^6 r^2} + \frac{3 \exp(-\beta r)}{4\beta^5 r} + \frac{\text{Ei}(-\beta r)}{4\beta^4},$$

$$f_{p1} = -\frac{2}{\beta r^2} + \frac{1}{r}, \quad f_{p2} = \frac{\exp(-\beta r)}{\beta^5 r^2} + \frac{\exp(-\beta r)}{2\beta^4 r},$$

$$f_{o3} = \frac{13}{16\beta^2} - \frac{5\gamma}{8\beta^2} + \frac{15 \exp(-\beta r)}{8\beta^4 r^2} + \frac{9 \exp(-\beta r)}{8\beta^3 r} + \frac{\text{Ei}(-\beta r)}{2\beta^2} - \frac{3\text{Ei}(-\beta r)}{4\beta^4 r^2} - \frac{5\Gamma(0, \beta r)}{8\beta^2} + \frac{r_p F_q[\{1, 1, 1\}; \{2, 2, 2\}; -\beta r]}{2\beta} + \frac{5 \ln(r)}{8\beta^2} - \frac{\gamma \ln(r)}{2\beta^2} + \frac{3 \exp(-\beta r) \ln(r)}{4\beta^4 r^2}$$

$$+ \frac{3 \exp(-\beta r) \ln(r)}{4\beta^3 r} - \frac{\text{Ei}(-\beta r) \ln(r)}{4\beta^2} - \frac{\Gamma(0, \beta r) \ln(r)}{2\beta^2} + \frac{\ln^2(r)}{4\beta^2} - \frac{5 \ln(\beta r)}{8\beta^2} - \frac{\ln(r) \ln(\beta r)}{2\beta^2}$$

$$f_{p3} = \frac{5 \exp(-\beta r)}{2\beta^3 r^2} + \frac{\exp(-\beta r)}{2\beta^2 r} - \frac{\text{Ei}(-\beta r)}{\beta^3 r^2} + \frac{\text{Ei}(-\beta r)}{2\beta^2 r} - \frac{\exp(-\beta r) \ln(r)}{\beta^3 r^2} + \frac{\exp(-\beta r) \ln(r)}{2\beta^2 r}$$

where $\text{Ei}(z) = -\int_{-z}^{\infty} \frac{e^{-t}}{t} dt$, γ Euler's constant = 0.577216, $\Gamma(a, z)$ the incomplete gamma function, ${}_pF_q(a; b; z)$ the generalized hypergeometric function [20] given by ${}_pF_q(a; b; z) = \sum_{k=0}^{\infty} (a_1)_k \cdots (a_p)_k / (b_1)_k \cdots (b_q)_k z^k / k!$.

References

- [1] Lekhnitskii SG. Theory of elasticity of an anisotropic body. Moscow: Mir Publishers; 1981.
- [2] Truesdell CA, Noll W. The nonlinear field theory of mechanics, Handbuch der Physik. Berlin: Springer; 1965. III/3.
- [3] Horgan CO, Chan AM. The pressurized hollow cylinder or disk problem for functionally graded isotropic linear elastic materials. J Elast 1999;55:43–59.
- [4] Tarn JQ. Exact solutions for functionally graded anisotropic cylinders subjected to thermal and mechanical loads. Int J Solids Struct 2001;38:8189–206.
- [5] Tarn JQ, Chang HH. Torsion of cylindrical orthotropic elastic circular bars with radial inhomogeneity: some exact solutions and end effects. Int J Solids Struct 2008;45:303–19.
- [6] Alshits VI, Kirchner HOK. Cylindrically anisotropic, radially inhomogeneous elastic materials. Proc Roy Soc Lond Ser A—Math Phys Eng Sci 2001;457:671–93.
- [7] Oral A, Anlas G. Effects of radially varying moduli on stress distribution of nonhomogeneous anisotropic cylindrical bodies. Int J Solids Struct 2005;42:5568–88.
- [8] Liew KM, Kitipornchai S, Zhang XZ, Lim CW. Analysis of the thermal stress behavior of functionally graded hollow circular cylinders. Int J Solids Struct 2003;44:2355–80.
- [9] Tutuncu N. Stresses in thick-walled FGM cylinders with exponentially-varying properties. Eng. Struct. 2007;29:2032–5.
- [10] Obata Y, Noda N. Steady thermal stresses in a hollow circular cylinder and a hollow sphere of a functionally graded material. J Therm Stress 1994;17:471–88.
- [11] Kim KS, Noda N. Green's function approach to unsteady thermal stresses in an infinite hollow cylinder of functionally graded material. Acta Mech 2002;156:145–61.
- [12] Pan E, Roy AK. A simple plane-strain solution for functionally graded multilayered isotropic cylinders. Struct Eng Mech 2006;24:727–40.
- [13] Shao ZS, Ma GW. Thermo-mechanical stresses in functionally graded circular hollow cylinder with linearly increasing boundary temperature. Compos Struct 2008;83:259–65.
- [14] Batra RC. Optimal design of functionally graded incompressible linear elastic cylinders and spheres. AIAA J 2008;46:2050–7.
- [15] Batra RC, Iaccarino GL. Exact solutions for radial deformations of a functionally graded isotropic and incompressible second-order elastic cylinder. Int J Non-Linear Mech 2008;43:383–98.
- [16] Batra RC. Finite plane strain deformations of rubberlike materials. Int J Numer Methods Eng 1980;15:145–60.
- [17] Batra RC, Bahrami A. Inflation and eversion of functionally graded nonlinear elastic incompressible circular cylinders. Int J Non-Linear Mech 2009;44:311–23.
- [18] Bilgili E. A parametric study of the circumferential shearing of rubber tubes: beyond isothermality and material inhomogeneity. Kaut Gummi Kunstst 2003;12:671–6.
- [19] Jabbari M, Sohrabpou S, Eslami MR. General solution for mechanical and thermal stresses in a functionally graded hollow cylinder due to nonaxisymmetric steady state loads. J Appl Mech – T ASME 2003;70:111–8.
- [20] Arfken G. Mathematical methods for physicists. 3rd ed. Orlando (FL): Academic Press; 1985.
- [21] Jiang B, Batra RC. Micromechanical modeling of composite containing piezoelectric and shape memory inclusions. J Intell Mater Syst 2001;12:165–82.
- [22] Nie GJ, Batra RC. Material tailoring and analysis of functionally graded isotropic and incompressible linear elastic hollow cylinders. Compos Struct 2010;92:265–74.
- [23] Batra RC. Torsion of a functionally graded cylinder. AIAA J 2006;44:1363–5.
- [24] Nie GJ, Batra RC. Stress analysis and material tailoring in isotropic linear thermoelastic incompressible functionally graded rotating disks of variable thickness. Compos Struct 2010;92:720–9.
- [25] Batra RC, Jin J. Natural frequencies of a functionally graded rectangular plate. J Sound Vibration 2005;282:509–16.